CHAPTER 9

Coherent Detection in the Infrared*

M. C. Teich

I. Introduction

Coherent (heterodyne) detection is well known in the radio wave, microwave, and optical[1–6] regions of the electromagnetic spectrum. Recently the

* This work was supported in part by the National Science Foundation.

[1] A. T. Forrester, R. A. Gudmundsen, and P. O. Johnson, *Phys. Rev.* **99**, 1691 (1955).

[2] A. E. Siegman, S. E. Harris, and B. J. McMurtry, *in* "Optical Masers" (J. Fox, ed.), p. 511. Wiley, New York, 1963.

[3] S. Jacobs, *Electronics* **36** (28), 29 (1963).

[4] M. E. Lasser, *Spectrum* **3**, 73 (1966).

[5] S. Jacobs and P. Rabinowitz, *in* "Quantum Electronics III" (P. Grivet and N. Bloembergen, eds.), p. 481. Columbia Univ. Press, New York, 1964.

[6] L. Mandel, *J. Opt. Soc. Am.* **56**, 1200 (1966).

M. C. Teich, "Coherent Detection in the Infrared," in Semiconductors and Semimetals, vol. 5, Infrared Detectors, edited by R. K. Willardson and A. C. Beer (Academic Press, New York, 1970), ch. 9, pp. 361-407.

technique has been extended to the middle infrared as well.[7–7b] This chapter discusses theoretical and experimental considerations related to coherent detection in the middle infrared, particularly at the 10.6 μ CO_2 laser wavelength.

Coherent detection differs in several significant respects from direct detection, or simple photon counting. In particular, the increased sensitivity available through its use in the infrared allows the detection of far weaker signals than by means of any other technique. The minimum detectable power corresponding to perfect quantum counting is $h\nu\,\Delta f$, the detection of one photon in every detector resolution time. Here $h\nu$ is the photon energy and Δf is the receiver bandwidth. The perfect quantum counter will detect each individual photon provided that the inverse photon count rate is large compared to the detector resolution time. For a real photoconductive and photovoltaic coherent detector the minimum detectable power is given by $(2/\eta)h\nu\,\Delta f$, rather than $h\nu\,\Delta f$, where η is the detector quantum efficiency. Thus a minimum of $2/\eta$ photons may be detected. Using a Ge:Cu photoconductive detector as few as five photons have been detected at 10.6 μ.[7]

A plot of the detectable number of photons vs the frequency of electromagnetic radiation from radio waves to X rays has been given by Townes[8] and is shown in Fig. 1. The peak in the curve at $\log_{10}\nu \approx 13.45$ (which is just $\nu \approx 2.83 \times 10^{13}$ Hz for the CO_2 laser) corresponds to the detection of very few photons in this region of the spectrum, and represents the results to be discussed in this chapter.

In the submillimeter region an improvement in sensitivity with heterodyne operation[9,10] has been demonstrated for InSb, pyroelectric, and Golay cell detectors. Using techniques similar to those described in this chapter, coherent detection experiments have been previously reported in the visible and the near infrared with photoemissive devices,[5,11] photodiodes,[2,12] and

[7] M. C. Teich, *Proc. IEEE* **56**, 37 (1968).

[7a] M. C. Teich, *Proc. IEEE* **57**, 786 (1969).

[7b] M. C. Teich, *Electron Technology* (to be published).

[8] C. H. Townes, Quantum Electronics, Past and Prospects, presented at the 1968 annual meeting of the Am. Phys. Soc., January 30, 1968. Also private communication.

[9] E. H. Putley, *Proc. IEEE (Correspondence)* **54**, 1096 (1966).

[10] H. A. Gebbie, N. W. B. Stone, E. H. Putley, and N. Shaw, *Nature* **214**, 165 (1967).

[11] A. E. Siegman, S. E. Harris, and B. J. McMurtry, *in* "Quantum Electronics III" (P. Grivet and N. Bloembergen, eds.), p. 1651. Columbia Univ. Press, New York, 1964; B. J. McMurtry and A. E. Siegman, *Appl. Opt.* **1**, 51 (1962).

[12] G. Lucovsky, M. E. Lasser, and R. B. Emmons, *Proc. IEEE* **51**, 166 (1963); G. Lucovsky, R. B. Emmons, B. Harned, and J. K. Powers, *in* "Quantum Electronics III" (P. Grivet and N. Bloembergen, eds.), p. 1731. Columbia Univ. Press, New York, 1964.

M. C. Teich, "Coherent Detection in the Infrared," in Semiconductors and Semimetals, vol. 5, Infrared Detectors, edited by R. K. Willardson and A. C. Beer (Academic Press, New York, 1970), ch. 9, pp. 361-407.

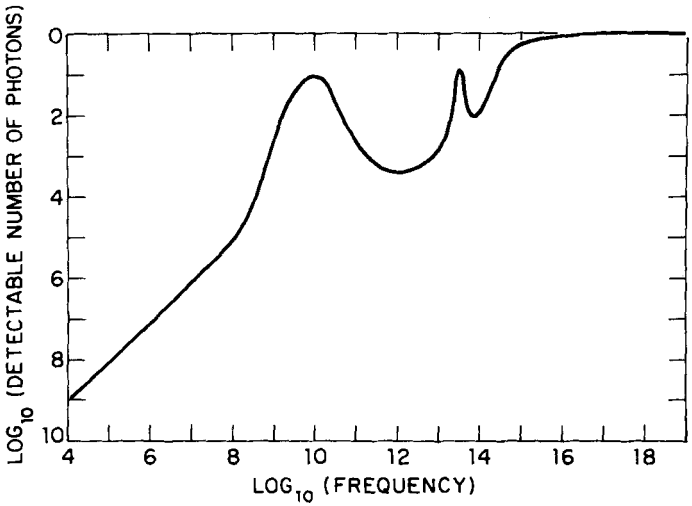

FIG. 1. Minimum detectable number of photons versus frequency from radio waves to X rays. The peak at $\log_{10} \nu \approx 13.45$ corresponds to optimum heterodyne detection at the CO_2 laser wavelength. (After Townes.[8])

photoconductors.[5,13,14] The use of an InAs diode has permitted heterodyne measurements to be extended to $3.5\,\mu$.[15] For frequencies $\geqslant 10^{16}$ Hz the large energy per photon makes it relatively easy to detect individual photons, so that the heterodyne technique is not particularly useful.

The configuration for a generalized heterodyne receiver in the optical or infrared is shown in Fig. 2. Its operation is made possible by the "nonlinear" response of the photodetector to the incident total radiation electric field. Two electromagnetic waves of different frequencies (ω_1 and ω_2) mix at the photodevice and produce an electrical signal with the difference frequency ($\omega_1 - \omega_2$). When one of these beams is made to be strong (if it is locally produced, it is then called the local oscillator or LO), the sensitivity for the process is considerably increased over the straight detection (video) case because of the high conversion gain between power at the input and at the difference frequencies.[2] In addition to this high conversion gain, the

[13] M. DiDomenico, Jr., R. H. Pantell, O. Svelto, and J. N. Weaver, *Appl. Phys. Letters* **1**, 77 (1962); R. H. Pantell, M. DiDomenico, Jr., O. Svelto, and J. N. Weaver, *in* "Quantum Electronics III" (P. Grivet and N. Bloembergen, eds.), Columbia Univ. Press, New York, 1964; G. Lucovsky, R. F. Schwartz, and R. B. Emmons, *Proc. IEEE (Correspondence)* **51**, 613 (1963).

[14] P. D. Coleman, R. C. Eden, and J. N. Weaver, *IEEE Trans. Electron Dev.* **11**, 488 (1964).

[15] F. E. Goodwin and M. E. Pedinoff, *Appl. Phys. Letters* **8**, 60 (1966).

M. C. Teich, "Coherent Detection in the Infrared," in Semiconductors and Semimetals, vol. 5, Infrared Detectors, edited by R. K. Willardson and A. C. Beer (Academic Press, New York, 1970), ch. 9, pp. 361-407.

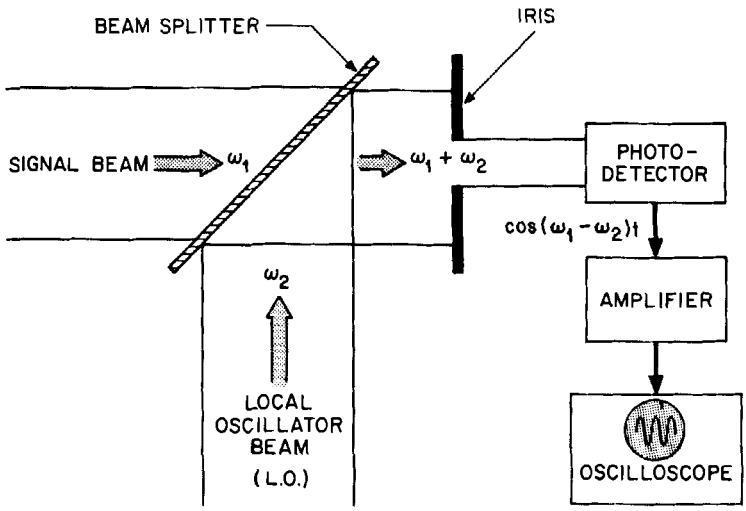

FIG. 2. The generalized infrared or optical heterodyne receiver. (After Teich.[7])

heterodyne detector exhibits both strong directivity and frequency selectivity. It is the frequency selectivity of the coherent detection process which permits the noise bandwidth to be reduced to a very small value. The heterodyne detector is linear only insofar as the detector output *power* is proportional to the input signal radiation *power*.

At optical and infrared frequencies the heterodyne detector acts as both an antenna and a receiver,[16] and has an integrated effective aperture limited by approximately λ^2. Careful alignment between the LO and signal beams is necessary in order to maintain a constant phase over the surface of the photodetector. The use of coherent detection in a communications system is therefore limited by the atmospheric distortion of the wavefront, which imposes a restriction on the maximum achievable signal-to-noise ratio.[17] Heterodyne detection is consequently most useful for detecting weak signals which are coherent with a locally produced source. It should be mentioned that the coherent detection technique is capable of furnishing information about the frequency spectrum of a signal beam.[6]

In the case where both the signal and the LO derive from the same source (such as in the experiments described in this chapter), the heterodyne signal can provide information about the velocity of a target through the Doppler shift. This is also possible if the LO and signal beams arise from different, but frequency locked, lasers.[3,6] Heterodyne detection is also useful for heterodyne spectroscopy[1,18] and in the study of physical processes occur-

[16] A. E. Siegman, *Proc. IEEE* **54**, 1350 (1966).
[17] D. L. Fried, *IEEE J. Quantum Electron.* **3**, 213 (1967); *Proc. IEEE* **55**, 57 (1967).
[18] H. Z. Cummins, N. Knable, and Y. Yeh, *Phys. Rev. Letters* **12**, 150 (1964).

M. C. Teich, "Coherent Detection in the Infrared," in Semiconductors and Semimetals, vol. 5, Infrared Detectors, edited by R. K. Willardson and A. C. Beer (Academic Press, New York, 1970), ch. 9, pp. 361-407.

ring in materials. Use of the technique has already been made in the design of a laser Doppler velocimeter, which measures localized flow velocities in gases and liquids.[19,20]

The measurements reported here have been performed at 10.6 μ in the middle infrared region. It is the availability of the high radiation power from the CO_2 laser together with the 8–14 μ atmospheric window[21] which make sensitive detection at 10.6 μ important for systems use. Furthermore, it is at these longer wavelengths that the higher sensitivity available from coherent detection is particularly valuable, since the user may discriminate against various noise sources including the blackbody radiation from objects at room temperature, which is appreciable at 10.6 μ. In the experiments reported below a minimum detectable radiation power which is within a factor of five of the theoretical quantum limit $h\nu\,\Delta f$ has been observed.

Because the setup employed in these experiments detects the scattered radiation from a diffusely reflecting moving surface, it is, in effect, a miniature prototype CO_2 laser radar. Thus, experiments on the power-spectral-density and the envelope probability distribution of the homodyne[21a] signal are also discussed. Use of the technique in a full-scale CO_2 laser radar, which has been recently set up and operated by Bostick,[22] is mentioned.

We begin with a discussion of the quantum theory of heterodyne detection and compare this with the classical theory. We then proceed to experimental results.

II. Quantum Theory of Infrared Coherent Detection

We present here a quantum theory of coherent detection which differs from both the classical and the semiclassical treatments. The theory, which has been applied over the entire electromagnetic spectrum,[23] reduces to the classical result in the limit of low radiation frequencies ($h\nu \ll kT$) and, for a certain class of fields, to the semiclassical result for high radiation frequencies ($h\nu \gg kT$). The primary distinction from the classical theory is that double-frequency and sum-frequency components do not appear in the heterodyne signal, to good approximation, when $h\nu \gg kT$, which is the region of interest for the work described here. The theory is valid for fields of an arbitrary statistical nature.

[19] Y. Yeh and H. Z. Cummins, *Appl. Phys. Letters* **4**, 176 (1964).

[20] J. W. Foreman, Jr., E. W. George, J. L. Jetton, R. D. Lewis, J. R. Thornton, and H. J. Watson, *IEEE J. Quantum Electron.* **2**, 260 (1966); R. D. Lewis, J. W. Foreman, Jr., H. J. Watson, and J. R. Thornton, *Phys. Fluids* **11**, 433 (1968).

[21] J. C. Stephenson, W. A. Haseltine, and C. B. Moore, *Appl. Phys. Letters* **11**, 164 (1967).

[21a] The terms homodyne and heterodyne are used interchangeably throughout this chapter.

[22] H. A. Bostick, *IEEE J. Quantum Electron.* **3**, 232 (1967).

[23] M. C. Teich, *Appl. Phys. Letters* **14**, 201 (1969); *J. Phys. Chem. Solids* (to be published).

M. C. Teich, "Coherent Detection in the Infrared," in Semiconductors and Semimetals, vol. 5, Infrared Detectors, edited by R. K. Willardson and A. C. Beer (Academic Press, New York, 1970), ch. 9, pp. 361-407.

1. Optical and Infrared Frequencies

A generalized schematic of the ordinary heterodyne receiver has been given in Fig. 2. Two plane parallel electromagnetic waves of frequencies ω_1 and ω_2 impinge normally on an ideal quantum-mechanical photodetector in its ground state. The detector has an energy level structure such that there is no excited state within an energy kT of the lowest level. This is a suitable assumption for the middle infrared or optical detector. It has been shown by Glauber[24,25] that the average count rate for such a detector at the space–time point $x_0 = \mathbf{r}_0, t_0$ may be expressed as the first-order correlation function $G^{(1)}_{\mu\nu}(x_0, x_0)$, where

$$G^{(1)}_{\mu\nu}(x_0, x_0) = \mathrm{tr}\{\rho E_\mu^-(x_0) E_\nu^+(x_0)\}, \tag{1}$$

with ρ the density operator for the field,[25,26] and E^- and E^+ the negative- and positive-frequency portions of the electric field operator, respectively. The subscripts μ, ν label Cartesian components. Only projections of the field along a single (possibly complex) unit vector are considered, so that the correlation function above may be written as a scalar quantity rather than as a tensor.

Coherent detection experiments are frequently performed using a given beam and a time-delayed form of the same beam[27] (so-called homodyne detection) so that it is more convenient to discuss field correlations relative to the radiation source rather than to the detector.[28] That is, the output of a detector illuminated by a single beam is proportional to $G^{(1)}(x', x')$, where $x' = \mathbf{r}, t'$. When illuminated by a phase-retarded form of the same beam the output of the detector *at time* t' may be written as $G^{(1)}(x'', x'')$ where $x'' = \mathbf{r}, t''$ and $t'' > t'$. Thus phase retardation is equivalent to time displacement at the detector, allowing for the coherence time to be considered as a parameter.

For the heterodyne experiment we may simply write the total electric field operator as a superposition of the operators for the constituent waves.[25] Therefore the positive-frequency component of the field present at the photodetector, $E^+(\mathbf{r}, t)$, may be written

$$E^+(\mathbf{r}, t) = \lambda_1 E^+(\mathbf{r}, t_1) + \lambda_2 E^+(\mathbf{r}, t_2). \tag{2}$$

The complex coefficients λ_1 and λ_2 contain the relative strengths of the two waves, and are taken to be independent of the properties of the field. The

[24] R. J. Glauber, *Phys. Rev.* **130**, 2529 (1963).

[25] R. J. Glauber, *in* "Quantum Optics and Electronics" (C. deWitt, A. Blandin, and C. Cohen-Tannoudji, eds.), p. 65. Gordon and Breach, New York, 1965.

[26] R. J. Glauber, *Phys. Rev.* **131**, 2766 (1963).

[27] S. Jacobs and P. Rabinowitz, *in* "Quantum Electronics III" (P. Grivet and N. Bloembergen, eds.), p. 481. Columbia Univ. Press, New York, 1964.

[28] M. C. Teich and G. J. Wolga, *Phys. Rev. Letters* **16**, 625 (1966).

M. C. Teich, "Coherent Detection in the Infrared," in Semiconductors and Semimetals, vol. 5, Infrared Detectors, edited by R. K. Willardson and A. C. Beer (Academic Press, New York, 1970), ch. 9, pp. 361-407.

count rate R may therefore be expressed as

$$R = \mathrm{tr}\{\rho E^-(\mathbf{r}, t)E^+(\mathbf{r}, t)\} = \mathrm{tr}\{\rho[\lambda_1^* E^-(x_1) + \lambda_2^* E^-(x_2)] \times [\lambda_1 E^+(x_1) + \lambda_2 E^+(x_2)]\}, \quad (3)$$

where, as above, the space–time point $x_1 = \mathbf{r}$, t_1 is relative to the radiation source. Using the correlation function identity[24]

$$[G^{(1)}(x_1, x_2)]^* = G^{(1)}(x_2, x_1), \quad (4)$$

this rate may be written in terms of the first-order time-dependent correlation functions $G^{(1)}(t_i, t_j)$ as

$$R = |\lambda_1|^2 G^{(1)}(t_1, t_1) + |\lambda_2|^2 G^{(1)}(t_2, t_2) + 2\,\mathrm{Re}\{\lambda_1^* \lambda_2 G^{(1)}(t_1, t_2)\}. \quad (5)$$

The first two terms on the right represent the intensities which would be contributed by each beam independently of the other; the last term represents the interference.

We have assumed that the angular alignment condition required for optimum photomixing is maintained,[29] so that the angle between the beams is restricted to a value smaller than λ/a, where λ is the radiation wavelength and a is the detector aperture. For this case the correlation function may be taken to vary slowly over the detector, and its spatial dependence suppressed, as above. We could, alternatively, retain the spatial dependence, in which case the condition for first-order coherence discussed in the next paragraph will automatically require the alignment condition to be fulfilled in order to obtain optimum photomixing.[23]

If the radiation incident on the detector possesses precise first-order coherence, two interesting consequences follow. The first relates to constraints on the correlation functions,[30] and will provide us with the magnitude of the heterodyne signal. The second concerns the density operator for the radiation field,[31] and will allow a physical interpretation for the beating process. The condition for maximum fringe contrast, or first-order coherence, has been shown by Titulaer and Glauber[30] to be equivalent to the factorization of the correlation function into two complex quantities $\mathscr{E}(t_1)$ and $\mathscr{E}(t_2)$:

$$G^{(1)}(t_1, t_2) = \mathscr{E}^*(t_1)\mathscr{E}(t_2). \quad (6)$$

With Eq. (5), under conditions of first-order coherence of the total incident radiation field,[23] we therefore obtain

$$R = |\lambda_1|^2 G^{(1)}(t_1, t_1) + |\lambda_2|^2 G^{(1)}(t_2, t_2) + 2\,\mathrm{Re}\{\lambda_1^* \mathscr{E}^*(t_1)\lambda_2 \mathscr{E}(t_2)\}. \quad (7)$$

[29] A. E. Siegman, *Appl. Opt.* **5**, 1588 (1966).
[30] U. M. Titulaer and R. J. Glauber, *Phys. Rev.* **140**, 3676 (1965).
[31] U. M. Titulaer and R. J. Glauber, *Phys. Rev.* **145**, 1041 (1966).

M. C. Teich, "Coherent Detection in the Infrared," in Semiconductors and Semimetals, vol. 5, Infrared Detectors, edited by R. K. Willardson and A. C. Beer (Academic Press, New York, 1970), ch. 9, pp. 361-407.

We may also write Eq. (5) in the equivalent form

$$R = |\lambda_1|^2 G^{(1)}(t_1, t_1) + |\lambda_2|^2 G^{(1)}(t_2, t_2) + 2|\lambda_1||\lambda_2||G^{(1)}(t_1, t_2)| \cos\{\phi(t_1, t_2) + \theta\}, \tag{8}$$

where $\phi(t_1, t_2)$ is a time-varying function derived from $G^{(1)}(t_1, t_2)$. The phase angle θ depends on the geometry of the experiment. While the first-order coherence condition has been used in obtaining Eq. (7), this is not so for the result in Eq. (8).

Using the correlation function equality[30] for first-order coherent fields,

$$|G^{(1)}(x_1, x_2)| = [G^{(1)}(x_1, x_1) G^{(1)}(x_2, x_2)]^{1/2}, \tag{9}$$

we obtain yet another expression for R,

$$R = |\lambda_1|^2 G^{(1)}(t_1, t_1) + |\lambda_2|^2 G^{(1)}(t_2, t_2) + 2[|\lambda_1|^2 G^{(1)}(t_1, t_1)|\lambda_2|^2 G^{(1)}(t_2, t_2)]^{1/2} \cos\{\phi(t_1, t_2)\}, \tag{10}$$

which is equivalent to Eq. (7) except for the (unimportant) suppression of θ. These results are valid for general fields (nonstationary as well as stationary) with arbitrary statistical properties (since only first-order correlation functions appear).

We now direct our attention to constituent beams which are stationary. Individual first-order coherence for these fields implies monochromaticity, and the functions $\mathscr{E}^*(t_1)$ and $\mathscr{E}(t_2)$ for well-collimated, fully-polarized beams (of frequency ω_1 and ω_2, respectively) may be expressed as[25]

$$\mathscr{E}^*(t_1) = [G^{(1)}(t_1, t_1)]^{1/2} \exp(i\omega_1 t_1) \tag{11}$$

and

$$\mathscr{E}(t_2) = [G^{(1)}(t_2, t_2)]^{1/2} \exp(-i\omega_2 t_2). \tag{12}$$

Here again the times t_1 and t_2 are relative to the source. Using these fields, the last term in Eq. (7) may be written

$$2\,\mathrm{Re}\{\lambda_1^* \mathscr{E}^*(t_1) \lambda_2 \mathscr{E}(t_2)\} = 2\,\mathrm{Re}\{\lambda_1^* \lambda_2 [G^{(1)}(t_1, t_1) G^{(1)}(t_2, t_2)]^{1/2} \times \exp(i\omega_1 t_1) \exp(-i\omega_2 t_2)\}. \tag{13}$$

Inserting the product $\exp(-i\omega_2 t_1) \exp(i\omega_2 t_1) \equiv 1$, we obtain

$$2\,\mathrm{Re}\{\lambda_1^* \mathscr{E}^*(t_1) \lambda_2 \mathscr{E}(t_2)\} = 2\,\mathrm{Re}\{\lambda_1^* \lambda_2 [G^{(1)}(t_1, t_1) G^{(1)}(t_2, t_2)]^{1/2} \times \exp[i(\omega_1 - \omega_2) t_1] \exp[i\omega_2 (t_1 - t_2)]\}. \tag{14}$$

M. C. Teich, "Coherent Detection in the Infrared," in Semiconductors and Semimetals, vol. 5, Infrared Detectors, edited by R. K. Willardson and A. C. Beer (Academic Press, New York, 1970), ch. 9, pp. 361-407.

For stationary constituent fields Eq. (7) thus becomes

$$R = |\lambda_1|^2 G^{(1)}(t_1, t_1) + |\lambda_2|^2 G^{(1)}(t_2, t_2) + 2[G^{(1)}(t_1, t_1) G^{(1)}(t_2, t_2)]^{1/2} \operatorname{Re}\{\lambda_1^* \lambda_2 \exp[i(\omega_1 - \omega_2)t_1] \exp(i\omega_2 \tau)\}, \tag{15}$$

where the quantity $\omega_2 \tau = \omega_2(t_1 - t_2)$ may be thought of as a phase difference between the beams.

Since we do not have advance information about the phase of a particular beam in any experiment, however, in using the theory we should properly choose states which are averaged over phase. Although the interference term in Eq. (15) will vanish through the ensemble average in this case, the interference would be present in any individual experiment. We assume that we can select an ensemble by considering only experiments with the same phase difference. This permissible procedure is entirely analogous to that used for spatial interference.[25] For convenience we shall choose the phase difference $\omega_2 \tau$ in such a manner as to precisely cancel the phase factors arising from λ_1^* and λ_2.

The counting rate for a restricted ensemble such as that discussed above, and for a field possessing first-order coherence with stationary constituent beams, may therefore finally be written as

$$R = |\lambda_1|^2 G^{(1)}(t_1, t_1) + |\lambda_2|^2 G^{(1)}(t_2, t_2) + 2[|\lambda_1|^2 G^{(1)}(t_1, t_1) |\lambda_2|^2 G^{(1)}(t_2, t_2)]^{1/2} \cos(\omega_1 - \omega_2)t. \tag{16}$$

The phase difference has been conveniently chosen as described above, and t_1 has been written as t in the interference term. We note that $G^{(1)}(t_1, t_1)$ and $G^{(1)}(t_2, t_2)$ are count rates which are constant in time and do not possess any fluctuating components. In terms of the classical intensities I_1 and I_2 for the individual beams this is equivalent to

$$R = I_1 + I_2 + 2(I_1 I_2)^{1/2} \cos(\omega_1 - \omega_2)t. \tag{17}$$

This expression differs from the usual classical result[3–5] in that it does not contain sum- and double-frequency components of ω_1 and ω_2. This will be made more explicit later. Although the correct result may be obtained semiclassically by using the analytic signal,[32] the range of validity of Eq. (17) (high frequencies such that $h\nu \gg kT$) appears naturally in the quantum treatment. Furthermore, the quantum theory may be used to obtain an expression valid throughout the electromagnetic spectrum,[23] as indicated earlier.

[32] L. Mandel and E. Wolf, *Rev. Mod. Phys.* **37**, 231 (1965).

M. C. Teich, "Coherent Detection in the Infrared," in Semiconductors and Semimetals, vol. 5, Infrared Detectors, edited by R. K. Willardson and A. C. Beer (Academic Press, New York, 1970), ch. 9, pp. 361-407.

It is observed from Eq. (10) that for nonstationary beams with a first-order coherent field the interference term exists but is not sinusoidal. The result in Eq. (5) is valid even when there is not maximum fringe contrast (first-order coherence). In that case, however, the equality in Eq. (9) no longer holds, and must be replaced by the inequality[30]

$$|G^{(1)}(x_1, x_2)| < [G^{(1)}(x_1, x_1)G^{(1)}(x_2, x_2)]^{1/2}. \tag{18}$$

From this it is evident that the photomixing term will be reduced below its maximum value when there is a departure from precise first-order coherence of the total incident radiation field. Thus, optimum sinusoidal photomixing is the result of temporal and spatial first-order coherence of the total incident radiation field, and stationarity of the constituent beams.[23]

a. Density Operator

The restriction which first-order coherence places on the density operator for the field has been discussed by Titulaer and Glauber.[31] They have generalized the definition of a mode to include nonmonochromatic solutions to the wave equation, and have thereby derived a density operator for the most general type of field possessing first-order coherence. This operator may be obtained by replacing the creation operator $a_k^\dagger$ in the single-mode density operator by a more general creation operator $b^\dagger$. This latter quantity creates a photon in a particular superposition of modes which may be considered as specifying a particular type of photon wave packet. Therefore a field which has first-order coherence may be regarded as consisting of photons of only a single (in general nonmonochromatic) variety. It has also been shown that if a field possesses such a density operator, it is first-order coherent. Since any field expressible in Glauber's P-representation may be separated into a coherent and an incoherent portion, furthermore, only the coherent portion will contain photons of the variety that give rise to a heterodyne signal.

The heterodyne detection process may then be considered as the annihilation of a single photon of this variety. Thus even in the presence of a single one of these photons a heterodyne signal may still be observed. As in the case of spatial interference,[33] therefore, Dirac's[34] well-known comment, "Each photon interferes only with itself. Interference between two different photons never occurs," applies to the heterodyne experiment. This is not surprising, since we are considering a type of interference experiment which is a one-quantum process. For multiple photon processes, such as two-

[33] R. L. Pfleegor and L. Mandel, *Phys. Rev.* **159**, 1084 (1967); *J. Opt. Soc. Am.* **58**, 946 (1968).
[34] P. A. M. Dirac, "Quantum Mechanics," 4th ed., Chap. I, p. 9. Oxford Univ. Press, London, 1958.

M. C. Teich, "Coherent Detection in the Infrared," in Semiconductors and Semimetals, vol. 5, Infrared Detectors, edited by R. K. Willardson and A. C. Beer (Academic Press, New York, 1970), ch. 9, pp. 361-407.

quantum detection[28,35–35b] or the Hanbury-Brown–Twiss effect, this is not necessarily true.[25]

b. Uncertainty Principle

The uncertainty principle also shows that it is not useful to consider the photons of the constituent beams separately. In fact, in a heterodyne experiment we are unable to determine from which beam a photon is absorbed in a given time interval. Consider a description in which there are two alternate ways in which the system can evolve from its initial state to the final state: by absorption of a photon from beam 1 or by absorption of a photon from beam 2. In order to ascertain which beam gave rise to the ejection of a particular photoelectron, its energy would have to be measured to within a value ΔE given by $\Delta E < \hbar|\omega_1 - \omega_2|$. From the uncertainty principle

$$\Delta E\, \Delta\tau \gtrsim \hbar, \tag{19}$$

the time $\Delta\tau$ required for such a measurement would be

$$\Delta\tau \gtrsim \hbar/\Delta E = |\omega_1 - \omega_2|^{-1}. \tag{20}$$

The required measurement time is greater than the period of the beat frequency, and such a measurement would therefore wash out the time interference. Thus one cannot ascribe a detected photon to one or the other of the constituent beams. A related argument has been applied by Pfleegor and Mandel[33] to independent beam spatial interference at the single-photon level.

c. Classical Theory

In the classical theory the total electric field vector E_t is given by

$$E_t = E_1 \cos(\omega_1 t) + E_2 \cos(\omega_2 t), \tag{21}$$

where E_1 and E_2 are the amplitudes of the individual incident waves. Assuming that E_1 and E_2 have the same polarization, the count rate R_c from the classical detector is proportional to the intensity of the radiation or to the square of the total electric field:

$$\begin{aligned} R_c = E_t^2 &= E_1^2 \cos^2(\omega_1 t) + E_2^2 \cos^2(\omega_2 t) \\ &\quad + E_1 E_2 \cos[(\omega_1 - \omega_2)t] + E_1 E_2 \cos[(\omega_1 + \omega_2)t]. \end{aligned} \tag{22}$$

The usual argument invoked at this point is that the detector cannot follow the instantaneous "intensity" at the sum- and double-frequency components if its resolution time is larger than the period of the radiation. Since the

[35] M. C. Teich and G. J. Wolga, *Phys. Rev.* **171**, 809 (1968).
[35a] M. C. Teich and P. Diament, *J. Appl. Phys.* **40**, 625 (1969).
[35b] P. Diament and M. C. Teich, *J. Opt. Soc. Am.* **59**, 661 (1969).

M. C. Teich, "Coherent Detection in the Infrared," in Semiconductors and Semimetals, vol. 5, Infrared Detectors, edited by R. K. Willardson and A. C. Beer (Academic Press, New York, 1970), ch. 9, pp. 361-407.

electron–photon correlation time[36] is $\sim 2 \times 10^{-14}$ sec in a metal, this provides a cutoff for the optical region. In any case, the post-detector circuitry generally has very limited frequency response, so that only averages of the first, second, and fourth terms in the above expression are observed. Thus such terms are usually ignored in the optical[1–5] and in the infrared,[7] and no contradiction with experiment is observed. However, it is clear from the quantum analysis that these rapidly varying terms never appear for the usual absorption detector when $h\nu \gg kT$, and therefore would not be observed even with detectors of arbitrarily small resolving time.

2. Signal-to-Noise Ratio

A parameter which is of interest in evaluating the usefulness of a receiving technique is the signal-to-noise ratio. In this section we discuss the operation of an infrared (optical) heterodyne receiver and calculate the expected signal-to-noise ratio at the output of the detector. Considering either the quantum theory or the classical theory with the usual assumptions, the response r of the detector to the two incident waves is given by

$$r = \beta\{\tfrac{1}{2}E_1^2 + \tfrac{1}{2}E_2^2 + E_1E_2\cos[(\omega_1 - \omega_2)t]\} = r_{dc} + r_{IF}, \tag{23}$$

where a proportionality factor β containing the quantum efficiency is now included (previously β was arbitrarily taken equal to 2). It is assumed that the detector has a sufficiently high frequency response to follow the signal at the difference frequency $(\omega_1 - \omega_2)$.

If we confine measurement of the signal to a band pass about the difference or heterodyne frequency (also called the intermediate frequency or IF), then it follows that

$$r_{IF} = \beta E_1E_2\cos[(\omega_1 - \omega_2)t]. \tag{24}$$

However, since $r_{dc} = \frac{1}{2}\beta(E_1^2 + E_2^2)$, the detector response may be written in terms of its dc component:

$$r = \left\{1 + \frac{2E_1E_2\cos[(\omega_1 - \omega_2)t]}{E_1^2 + E_2^2}\right\} r_{dc}. \tag{25}$$

For a very strong LO beam, which is the usual experimental condition, $E_2 \gg E_1$, and it follows that

$$r_{IF} = 2(E_1/E_2)r_{dc}\cos(\omega_{IF}t). \tag{26}$$

The mean-square photodetector response for a sinusoidal signal is then given by

$$\langle r_{IF}^2\rangle = 2(P_1/P_2)r_{dc}^2, \tag{27}$$

where P_1 and P_2 are the radiation powers in the signal beam and LO beam, respectively.

[36] P. S. Pershan and N. Bloembergen, *Appl. Phys. Letters* **2**, 117 (1963).

M. C. Teich, "Coherent Detection in the Infrared," in Semiconductors and Semimetals, vol. 5, Infrared Detectors, edited by R. K. Willardson and A. C. Beer (Academic Press, New York, 1970), ch. 9, pp. 361-407.

a. Photoemitter and Ideal Reverse-Biased Photodiode

If we now consider the noise response r_n in the detector as arising from shot noise,[37,38] which is the case for the photoemitter and the ideal reverse-biased photodiode, then the mean-square noise response is given by the well-known shot-noise formula

$$\langle r_n^2 \rangle = 2er_{dc}\,\Delta f, \tag{28}$$

where Δf is the bandwidth of the receiver. Hence the signal-to-noise ratio $(S/N)_{power}$ may be written

$$(S/N)_{power} = \frac{\langle r_{IF}^2 \rangle}{\langle r_n^2 \rangle} = \frac{P_1}{e\,\Delta f}\left(\frac{r_{dc}}{P_2}\right). \tag{29}$$

However, since r_{dc} arises from the comparatively large LO, it is related to the LO beam power P_2 by the quantum efficiency η:

$$r_{dc} = (\eta e/h\nu)P_2. \tag{30}$$

Thus, for a sinusoidal signal, the signal-to-noise ratio becomes[37,38]

$$(S/N)_{power} = \eta P_1/h\nu\,\Delta f \quad \text{(photoemitter and reverse-biased photodiode).} \tag{31a}$$

From this relation it is seen that the value of the signal-beam radiation power necessary to achieve a $(S/N)_{power} = 1$ is given by

$$P_s^{min} = h\nu\,\Delta f/\eta \quad \text{(photoemitter and reverse-biased photodiode).} \tag{31b}$$

This quantity is defined as the minimum detectable power, and is denoted by P_s^{min}. It has been assumed that experimental conditions are such that the "excess noise"[39–40a] above shot noise may be neglected. This is usually, but not always, true for single-mode laser sources operating well above threshold, where intensity fluctuations are quieted.

If the two radiation beams impinging on the detector are not parallel to within a certain angular tolerance,[16,41] and do not illuminate the same area, or the radiation is not normally incident upon the photodetector,[42] then (S/N) and P_s^{min} will differ from expressions in Eqs. (31a) and (31b). The radiation beam incident on the detector must also possess first-order coherence for this result to hold.[23] In the experiments reported in this work the conditions required for the relations given in Eqs. (31a) and (31b) have

[37] B. M. Oliver, *Proc. I.R.E. (Correspondence)* **49**, 1960 (1961).

[38] H. A. Haus, C. H. Townes, and B. M. Oliver, *Proc. I.R.E. (Correspondence)* **50**, 1544 (1962).

[39] C. Freed and H. A. Haus, *Phys. Rev.* **141**, 287 (1966).

[40] J. A. Armstrong and A. W. Smith, *in* "Progress in Optics" (E. Wolf, ed.), p. 213. North–Holland Pub., Amsterdam, 1967.

[40a] J. J. Mezrich, Circuit Model for Amplitude Noise in Lasers. M.S. thesis, Massachusetts Institute of Technology, Cambridge, Massachussetts, January 1969 (unpublished).

[41] V. J. Corcoran, *J. Appl. Phys.* **36**, 1819 (1965).

[42] A. J. Bahr, *Proc. IEEE (Correspondence)* **53**, 513 (1965).

M. C. Teich, "Coherent Detection in the Infrared," in Semiconductors and Semimetals, vol. 5, Infrared Detectors, edited by R. K. Willardson and A. C. Beer (Academic Press, New York, 1970), ch. 9, pp. 361-407.

been satisfied. For a sufficiently large LO power the theory derived in the form given above has been experimentally verified both for the case of photoemitters[5] and for back-biased photodiodes.[12,15] In particular, Hanlon and Jacobs[43] have recently verified Eqs. (31a) and (31b) in a bandwidth of 1 Hz using an InAs diode detector.

b. Photoconductor and Photovoltaic Diode

For the case of a photoconductor the noise behavior differs from simple shot noise, and the results derived above are not directly applicable. Photoconductor noise is a complicated phenomenon,[44] and depends to a great extent on the nature of the photoconductor.[44a] In the limit of large LO powers, however, extrinsic Ge:Cu is expected to display simple generation–recombination (g–r) noise.[45] Since the behavior for simple g–r noise is the same as that for shot noise except for a factor of two,[14,45–47] it may be shown that the signal-to-noise ratio for Ge:Cu has a value just one-half as large as that for a photoemitter or a nonleaky reverse-biased photodiode of the same quantum efficiency. The same result has also been obtained as a special case (in the absence of trapping) of a relation derived by DiDomenico and Anderson[48] for CdSe.

In the photovoltaic cell, on the other hand, the same processes occur as in the reversed-biased photodiode. However, instead of generating a current, a voltage results from the dipole-layer charge, since the cell is effectively open circuited. The detectivity and the real noise equivalent power (RNEP) for both the reverse-biased p–n junction and the photovoltaic detector have recently been discussed by van Vliet,[44] who has shown that the RNEP for the photovoltaic cell is higher than that for the reverse-biased photodiode by a factor of $\sqrt{2}$. It follows that the (electronic) noise power, which is proportional to the square of the RNEP, is a factor of two greater for the photovoltaic configuration. Therefore the signal-to-noise ratio for the photovoltaic device, as for the photoconductor, is just one-half that for the photoemitter or the reverse-biased photodiode. It should be pointed out, however, that the advantage gained in signal-to-noise ratio for reverse-

[43] J. Hanlon and S. F. Jacobs, *IEEE J. Quantum Electron.* **3**, 242 (1967).

[44] K. M. van Vliet, *Appl. Opt.* **6**, 1145 (1967).

[44a] Van Vliet[44] has separated photoconductors into four classes, each of which behaves differently: intrinsic, minority trapping model, two-center model, and extrinsic.

[45] H. Levinstein, *Appl. Opt.* **4**, 639 (1965).

[46] R. C. Jones, *Proc. I.R.E.* **47**, 1841 (1959).

[47] A. van der Ziel, "Fluctuation Phenomena in Semi-Conductors," pp. 22, 65. Butterworths, London and Academic Press, New York, 1959.

[48] M. DiDomenico, Jr. and L. K. Anderson, Signal-to-Noise Performance of CdSe Bulk Photoconductive Detectors. Bell Telephone Lab., Murray Hill, New Jersey (unpublished memorandum).

M. C. Teich, "Coherent Detection in the Infrared," in Semiconductors and Semimetals, vol. 5, Infrared Detectors, edited by R. K. Willardson and A. C. Beer (Academic Press, New York, 1970), ch. 9, pp. 361-407.

biased photodiode operation can only be realized for detectors having a high reverse-bias dynamic resistance, as will be seen later.

The signal-to-noise ratio and minimum detectable power for the extrinsic photoconductor and for the photovoltaic junction are therefore given by

$$(S/N)_{\text{power}} = \eta P_1/2h\nu\,\Delta f, \quad \text{(photoconductor and photovoltaic diode).} \tag{32a}$$

$$P_s^{\min} = (2/\eta)h\nu\,\Delta f. \tag{32b}$$

These devices are a factor of two less sensitive than a photoemitter or ideal reverse-biased photojunction of the same quantum efficiency [compare Eqs. (31a) and (31b)], and a factor of $2/\eta$ less sensitive than the perfect quantum counter. (For the photoconductor, although both the signal and the noise depend on the photoconductor gain G, the ratio may be shown to be independent of this parameter.[13])

The operation of photoconductive Ge:Cu as a heterodyne detector near the theoretical limit given by Eqs. (32a) and (32b) was demonstrated by Teich *et al.*[49] Similar experiments performed on Ge:Hg by Buczek and Picus[50] have also been found to agree closely with the predictions of Eqs. (32a) and (32b).

In later sections we discuss in detail the experimental results of heterodyne measurements on photoconductive Ge:Cu and on photovoltaic $Pb_{1-x}Sn_xSe$. In both of these cases the experimental agreement with the theory outlined in this section is quite good. It should be kept in mind, nonetheless, that the expressions given here have been derived explicitly for a *sinusoidal* heterodyne signal.

III. Measurement of the Signal-to-Noise Ratio

3. Experimental Arrangement

A block diagram of the experimental arrangement used for the heterodyne measurements[7,49] in photoconductive Ge:Cu is shown in Fig. 3. The radiation from a CO_2–N_2–He laser, with an output power of approximately 10 W at 10.6 μ, was incident on a modified Michelson interferometer. One mirror of the conventional interferometer was replaced by an off-center rotating aluminum wheel which had a roughened edge obtained by sandblasting.

The diffusely scattered radiation from the wheel provided a Doppler-shifted signal which was recombined at the beamsplitter with the unshifted

[49] M. C. Teich, R. J. Keyes, and R. H. Kingston, *Appl. Phys. Letters* **9**, 357 (1966).

[50] C. J. Buczek and G. S. Picus, *Appl. Phys. Letters* **11**, 125 (1967); G. S. Picus and C. J. Buczek, Far Infrared Laser Receiver Investigation. Hughes Res. Lab., Malibu, California, Interim Tech. Rept. No. 4, Contract AF33(615)-3487, 1967 (see also Repts. 1–3).

M. C. Teich, "Coherent Detection in the Infrared," in Semiconductors and Semimetals, vol. 5, Infrared Detectors, edited by R. K. Willardson and A. C. Beer (Academic Press, New York, 1970), ch. 9, pp. 361-407.

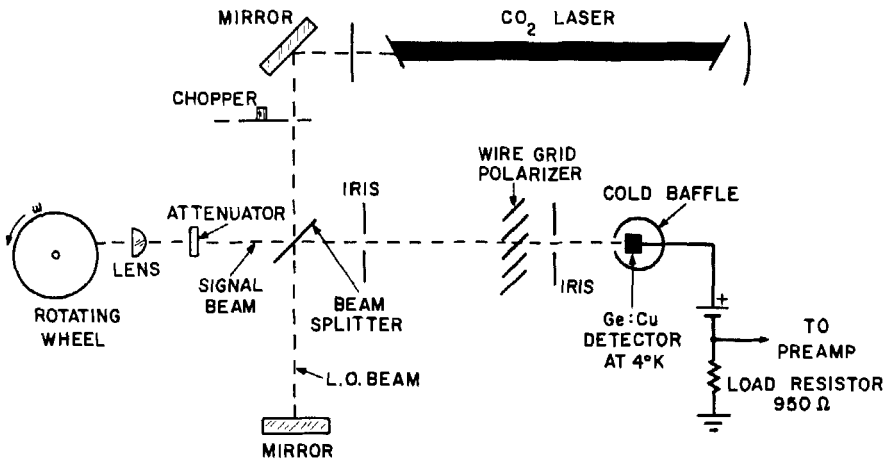

FIG. 3. Experimental arrangement for heterodyne measurements with a Ge:Cu detector. The electric field vector lies perpendicular to the plane of the paper. (After Teich.[7])

LO radiation reflected from the mirror of the other interferometer leg. Both the mirror and the beamsplitter were cocked at a slight angle to the usual 90° and 45° (respectively) in order to prevent this reflected radiation from feeding back into the laser. Heterodyne detection measurements with scattered radiation at 0.6328 μ have been made previously by Gould *et al.*[51] and by others.[52] A. E. Siegman has calculated the maximum radiation power to be returned by a random scatterer.[16,53]

The experimental apparatus, with the exception of the rotating wheel and the chopper, was mounted on a granite slab supported by compressed fiberglass blocks. To further reduce the effect of acoustic vibrations the 1.25-m-long Brewster window sealed laser tube was set on shock mounts and enclosed in a wooden shield paneled with acoustic tile. The laser was operated well above threshold and was very carefully tuned to operate on a single line and mode, so that no excess noise (above shot noise) was expected from the beam. This was accomplished by blocking the signal beam and then adjusting one laser mirror for a TEM_{00} mode and the absence of any observable beat signal. The interferometer mirror was then adjusted to give the largest signal-to-noise ratio when the signal beam was permitted to pass. Back and forth adjustments were made until a mirror position was found for which all of the above conditions were coincident. An uncoated Irtran II flat (of thickness 0.64 cm) served as a beamsplitter, and front surface

[51] G. Gould, S. F. Jacobs, J. T. LaTourette, M. Newstein, and P. Rabinowitz, *Appl. Opt.* **3**, 648 (1964).

[52] R. D. Kroeger, *Proc. IEEE (Correspondence)* **53**, 211 (1965); G. A. Massey, *Appl. Opt.* **4**, 781 (1965).

[53] A. E. Siegman, *IEEE Trans. Antennas Propagation* **15**, 192 (1967).

M. C. Teich, "Coherent Detection in the Infrared," in Semiconductors and Semimetals, vol. 5, Infrared Detectors, edited by R. K. Willardson and A. C. Beer (Academic Press, New York, 1970), ch. 9, pp. 361-407.

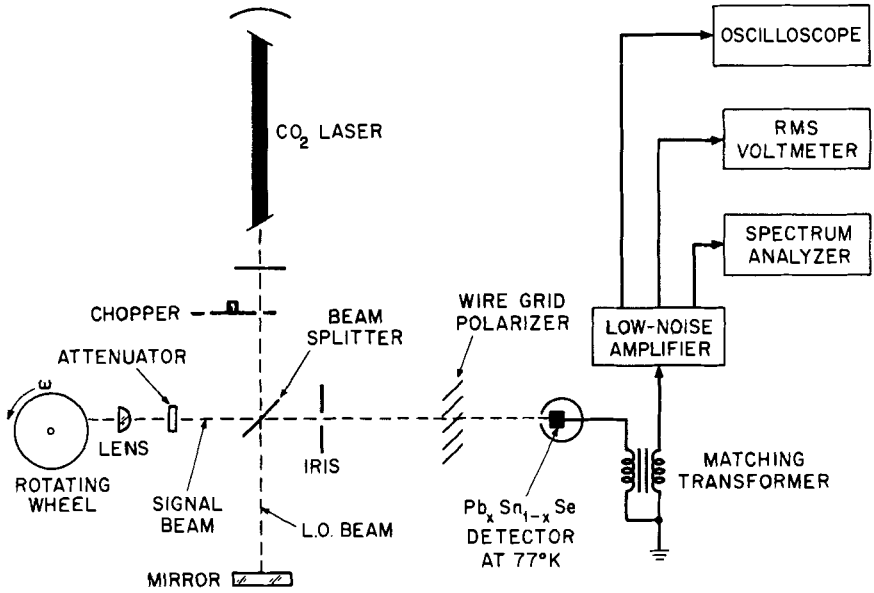

FIG. 4. Experimental arrangement for measurements with a $Pb_{1-x}Sn_xSe$ detector. The arrangement is similar to that shown in Fig. 3, with the exception of the detector output circuitry. (After Teich.[7])

mirrors were of standard aluminum-coated glass. These mirrors were highly reflective in order to prevent thermal distortion and consequent deformation of the wavefront of the reflected radiation.

An Irtran II lens of focal length 2.54 cm was inserted in the signal beam to focus the radiation to a single point on the sandblasted rim of the rotating wheel. The purpose of the lens was twofold: It served to collect sufficient scattered radiation to permit an incoherent (nonheterodyne) measurement of the scattered signal power at the detector for calibration purposes, and it also ensured spatial coherence of the scattered radiation over the receiver aperture. This is analogous to the technique used to obtain spatially coherent thermal radiation, where the source is focused onto a pinhole aperture stop. This ensures that all points on the wavefront emanating from the pinhole arise from the same source point and are therefore correlated. The coherence properties may be deduced from the van Cittert–Zernike theorem.[51,54]

Irises were used to maintain the angular alignment of the wavefronts of the two beams to within λ/a, the required angular tolerance for optimum photomixing (a is the detector aperture).[16] It should be noted that this angular alignment restriction is 20 times less stringent than in the visible region of the spectrum. A Perkin–Elmer wire-grid polarizer ensured that the

[54] M. Born and E. Wolf, "Principles of Optics," p. 505. Pergamon Press, Oxford, 1959.

M. C. Teich, "Coherent Detection in the Infrared," in Semiconductors and Semimetals, vol. 5, Infrared Detectors, edited by R. K. Willardson and A. C. Beer (Academic Press, New York, 1970), ch. 9, pp. 361-407.

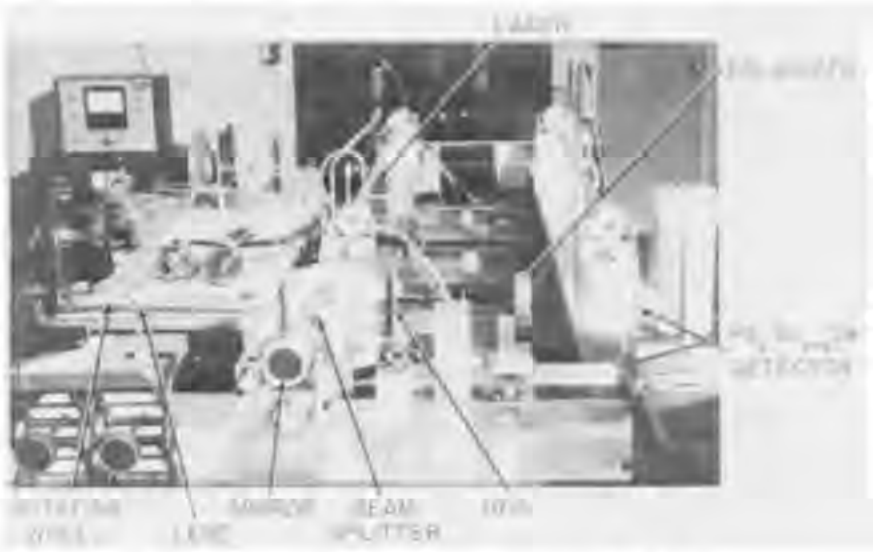

FIG. 5. Photograph of the heterodyne apparatus. (After Teich.[7])

recombined beams, which impinged normally on the photodetector, had a common linear polarization. The output from the detector was fed through a controlled-bandwidth, low-noise amplifier to a thermocouple-type rms voltmeter. Alternately, the signal was fed simultaneously to an oscilloscope and to a spectrum analyzer.

The setup used for the heterodyne measurements with photovoltaic $Pb_{1-x}Sn_xSe$ is shown in Fig. 4. It is essentially identical to the arrangement for Ge:Cu, with the notable exception of the detector output circuitry. For the high-impedance photoconductor (dark resistance ~ 600 kilohms) a 1-kilohm load resistor is used to convert the photocurrent to a voltage suitable for amplification. For the low-impedance photovoltaic device (~ 1.5 ohms), on the other hand, the voltage is both increased and transformed in impedance by the use of a matching transformer. A photograph of the actual apparatus used in these measurements is shown in Fig. 5.

4. EXPERIMENTS WITH PHOTOCONDUCTIVE GE:CU

a. Detector Fabrication and Characteristics

The copper-doped germanium detectors used in the heterodyne experiments were made by indiffusion of Cu into high-resistivity *n*-type germanium host material for a period of 16 hr at 760°C. The samples, which were

M. C. Teich, "Coherent Detection in the Infrared," in Semiconductors and Semimetals, vol. 5, Infrared Detectors, edited by R. K. Willardson and A. C. Beer (Academic Press, New York, 1970), ch. 9, pp. 361-407.

2 mm × 2.2 mm × 3 mm in size were then quenched in air. The resulting copper atom concentration was $6.8 \times 10^{15}\,cm^{-3}$, and the compensation by the original donors was such as to produce a free-hole lifetime of about 2×10^{-9} sec at 4°K. With a bias voltage of 13.5 V on the detector its (incoherent) low-power responsivity was 0.2 A/W by calibration with a blackbody source of known temperature. The detector was operated near liquid helium temperature.

b. Heterodyne Operation at kHz Frequencies

Figure 6(a) shows a multiple-sweep display of the heterodyne signal obtained at the detector output with a signal beam radiation power of 1×10^{-8} W. The loss of definition of the waveform in the third cycle reflects the finite bandwidth of the heterodyne signal. Figure 6(b) shows a single trace of this signal for a longer time scale. The modulation bandwidth is caused by statistical fluctuations of the heterodyne signal arising from the moving diffuse surface of the wheel.

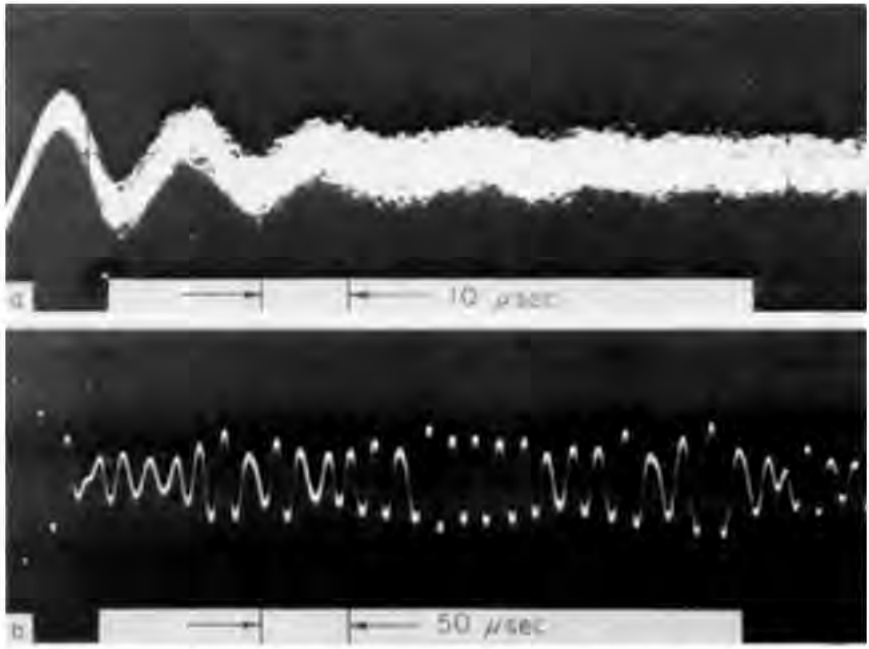

FIG. 6. (a) A multiple-sweep display of the heterodyne signal from a Ge:Cu detector. The loss of definition of the waveform in the third cycle reflects the finite bandwidth of the heterodyne signal. (b) A single-sweep of the signal shown in (a), but with a longer time scale. The modulation of the signal envelope arises from the random nature of the scattering surface. (After Teich.[7])

M. C. Teich, "Coherent Detection in the Infrared," in Semiconductors and Semimetals, vol. 5, Infrared Detectors, edited by R. K. Willardson and A. C. Beer (Academic Press, New York, 1970), ch. 9, pp. 361-407.

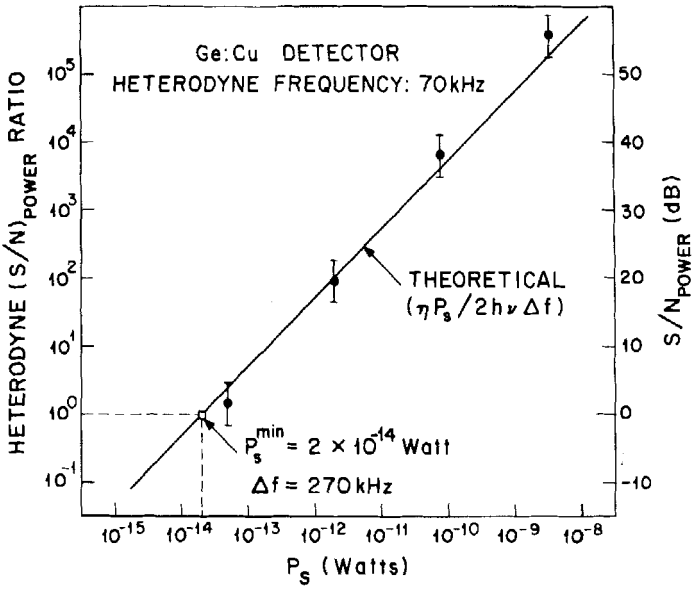

FIG. 7. The data points, obtained from a typical run, represent the observed signal-to-noise ratio of the heterodyne signal in Ge:Cu, $(S/N)_{power}$, for a given signal-beam radiation power (P_s). The theoretical curve, given by the expression $(S/N)_{power} = \eta P_s/2h\nu\,\Delta f$, is in good agreement with the data. The minimum detectable power P_s^{min} (defined as that signal beam power for which the heterodyne S/N is unity) corresponds, in a 1-Hz bandwidth, to 7×10^{-20} W. (After Teich.[7])

The results of a typical experimental measurement of the heterodyne signal-to-noise ratio for the detector are shown in Fig. 7. The filled circles represent the observed signal-to-noise power ratio data points, $(S/N)_{power}$, as a function of the signal beam radiation power (P_s or P_1). Only noise arising from the presence of the single-mode, single-frequency LO beam (which was the dominant contribution to the noise) is considered. Various values of P_s were obtained by inserting calibrated CaF_2 attenuators in the signal beam, while the unattenuated power was measured by chopping the signal beam in the absence of the LO. As indicated earlier, the presence of the lens facilitated this measurement.

A plot of the theoretically expected result for a sinusoidal signal [Eq. (32a)],

$$(S/N)_{power} = \eta P_s/2h\nu\,\Delta f, \tag{33}$$

is also shown in Fig. 7. Using an estimated quantum efficiency $\eta = \frac{1}{2}$, it is in good agreement with the experimental data. Had noise from sources other than the LO been taken into account in computing the S/N, the

M. C. Teich, "Coherent Detection in the Infrared," in Semiconductors and Semimetals, vol. 5, Infrared Detectors, edited by R. K. Willardson and A. C. Beer (Academic Press, New York, 1970), ch. 9, pp. 361-407.

experimental values would still be within a factor of two of the theoretical curve. Measurements were made with an LO power of 1.5 mW.

With a heterodyne signal centered at about 70 kHz and an amplifier bandwidth of 270 kHz the experimentally observed minimum detectable power $P_s^{\min}$ (defined as that signal beam power for which the heterodyne S/N is unity) was 2×10^{-14} W. In a 1-Hz bandwidth this corresponds to a minimum detectable power of 7×10^{-20} W, which is to be compared with the expected value

$$(2/\eta)h\nu\,\Delta f \approx 7.6 \times 10^{-20} \quad \text{W}. \tag{34}$$

The experimental measurement is therefore within 6 dB of the theoretically perfect quantum counter, and is in substantial agreement with the expected result for the Ge:Cu detector used in the experiments.

c. Noise Modulation

Because the roughness of the wheel ($\sim 10\,\mu$) is comparable to the radiation wavelength λ, the bandwidth of the noise modulation B should be given by[49]

$$B \sim v/d, \tag{35}$$

where v is the velocity at which the illuminated spot traverses the surface and d is the diameter of the focused spot on the wheel ($\sim 50\,\mu$). This follows from the fact that every d/v seconds a completely new spot on the wheel is illuminated, giving rise to scattered radiation which is uncorrelated with that of the previous time interval. The coherence time τ_1 is therefore

$$\tau_1 \sim d/v, \tag{36}$$

since the frequency bandwidth is given by the inverse coherence time. With

$$v = r\dot{\theta} \tag{37}$$

and

$$d \approx F\lambda/D, \tag{38}$$

the noise-modulation bandwidth is given approximately by

$$B \sim r\dot{\theta}D/F\lambda. \tag{39}$$

Here v is the tangential velocity of the wheel (157 cm/sec), $\dot{\theta}$ is its angular velocity (10π sec^{-1}), and r its radius (5.05 cm); F represents the focal length of the lens (2.54 cm), while D is the diameter of the radiation beam at the output of the laser (~ 5 mm).

Using these values, a calculated noise modulation bandwidth

$$B \sim 30 \quad \text{kHz} \tag{40}$$

M. C. Teich, "Coherent Detection in the Infrared," in Semiconductors and Semimetals, vol. 5, Infrared Detectors, edited by R. K. Willardson and A. C. Beer (Academic Press, New York, 1970), ch. 9, pp. 361-407.

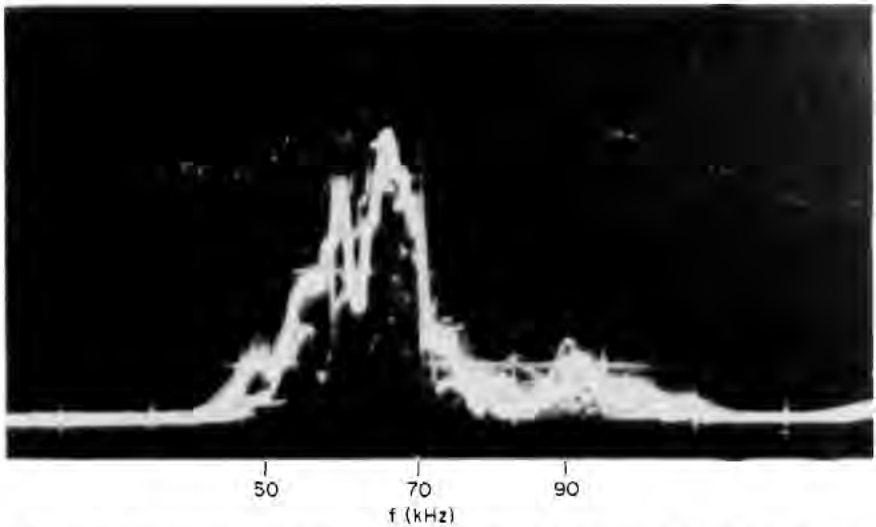

FIG. 8. A typical power-spectral-density trace of the heterodyne signal from Ge:Cu. The trace sweep speed was 4 sec^{-1}. The center frequency of 70 kHz corresponds to the period of 14 μsec observed in Fig. 6(b). (After Teich.[7])

is obtained which is comparable with the value observed on the power-spectral-density trace shown in Fig. 8. A Panoramic model SB-15a ultrasonic spectrum analyzer operated with a trace sweep speed of $\approx 4\ sec^{-1}$ was used for the observations. A smooth, bell-shaped curve would have been obtained by integrating and then recording the power-spectral-density curve. The center frequency of 70 kHz corresponds to the period of 14 μsec observed in Fig. 6(b). Both traces were obtained directly across the (1 kilohm) photoconductor load resistor. A more detailed treatment of the power-spectral-density will be given later.

d. Possible Power Dependence of Photoconductor Gain

A discrepancy between the observed values of signal and noise (individually, rather than the ratio) when compared with the values calculated on the basis of the measured responsivity has not been resolved.[49] Experiments have shown, however, that the photoconductor gain depends neither on the chopping frequency of the incident radiation nor on the heterodyne frequency, a possible cause for the disagreement. Other experiments, which were performed by placing attenuators in various positions in the optical path, indicate that amplification of frequency-shifted (scattered) radiation[55] by the laser is not responsible for the effect. Measurements of the small-signal

[55] W. M. Doyle, W. D. Gerber, and M. B. White, *IEEE J. Quantum Electron.* 3, 479 (1966).

photoconductor gain as a function of the LO power were inconclusive, and it remains possible that this effect has some bearing on the problem. It appears that this discrepancy does not occur for the lead-tin selenide photodiode detectors.

e. Results for Other Materials at $10.6\,\mu$

The results discussed in this section are similar to those given for Ge:Cu by Teich *et al.*[7,49] Buczek and Picus[50] in their experiments with Ge:Hg used two independent CO_2 lasers oscillating at slightly different frequencies. The minimum detectable power which they obtained (referred to a 1-Hz bandwidth) was

$$P_s^{\min}(\text{Ge:Hg}) = 1.73 \times 10^{-19}\,\text{W}, \tag{41}$$

which is in good agreement with the results obtained for Ge:Cu using a completely different experimental configuration. More recently, Mocker[55a] has also achieved operation near the theoretical limit in photoconductive $Cd_xHg_{1-x}Te$, while Leiba[55b] and Abrams and Glass[55c] have observed the effect in pyroelectric triglycine sulphate (TGS) and in $Sr_{1-x}Ba_xNb_2O_6$ (SBN), respectively.

5. Experiments with Photovoltaic $Pb_{1-x}Sn_xSe$

a. Detector Fabrication

The $Pb_{1-x}Sn_xSe$ diodes used as heterodyne detectors were fabricated from Bridgman-grown crystals by Melngailis and by Calawa *et al.*[56–58] The band gap of these diffused p–n junction devices varies with composition (x), so that the wavelength for peak responsivity may be adjusted by varying x. The devices which were used achieved their maximum responsivity (~ 1 V/W, 77°K) at the CO_2-laser wavelength, and had the composition $Pb_{0.936}Sn_{0.064}Se$ (see Fig. 9 for a plot of the responsivity versus wavelength for a typical diode). The nature and inversion properties of the conduction and valence bands for these alloys have been discussed in detail both for the diodes[56–58] and for single-crystal thin films.[59] The inversion behavior of

[55a] H. Mocker, *Appl. Opt.* **8**, 677 (1969).
[55b] E. Leiba, *Compt. Rend.* **268B**, 31 (1969).
[55c] R. L. Abrams and A. Glass, *Appl. Phys. Letters* **15**, 251 (1969).
[56] I. Melngailis, unpublished work (1967).
[57] A. R. Calawa, I. Melngailis, T. C. Harman, and J. O. Dimmock, Photovoltaic Response of $Pb_{1-x}Sn_xSe$ Diodes, presented at the Solid State Device Res. Conf., Univ. of Calif. at Santa Barbara, June 19–21, 1967.
[58] J. F. Butler, A. R. Calawa, I. Melngailis, T. C. Harman, and J. O. Dimmock, *Bull. Am. Phys. Soc.* **12**, 384 (1967).
[59] A. J. Strauss, *Phys. Rev.* **157**, 608 (1967).

M. C. Teich, "Coherent Detection in the Infrared," in Semiconductors and Semimetals, vol. 5, Infrared Detectors, edited by R. K. Willardson and A. C. Beer (Academic Press, New York, 1970), ch. 9, pp. 361-407.

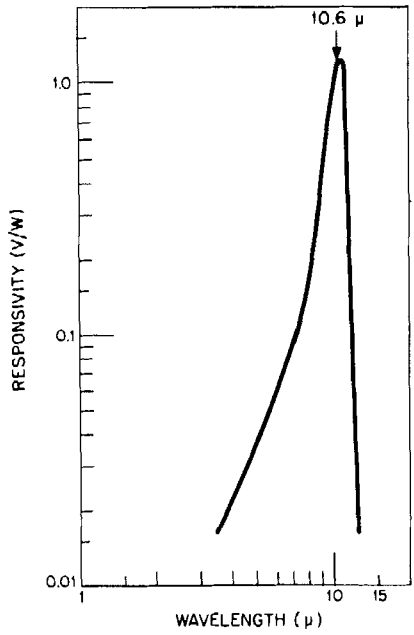

FIG. 9. Responsivity of a typical $Pb_{0.936}Sn_{0.064}Se$ diode versus wavelength at 77°K. (After Melngailis.[56])

the bands in $Pb_{1-x}Sn_xSe$ is similar to that observed for $Pb_{1-x}Sn_xTe$.[60] The detectivity of the devices D^* was

$$D^* > 3 \times 10^9 \quad \text{cm sec}^{-1/2}\,\text{W}^{-1} \tag{42}$$

and the carrier concentration was $\sim 10^{17}\,\text{cm}^{-3}$.

b. Device Characteristics

The diodes had a 1-mm diameter active area and were operated at 77°K in the photovoltaic mode. The thin n-type layer ($\sim 10\,\mu$) was exposed to the LO and signal beam radiation. The I–V characteristic of diode #37, both in the absence and in the presence of the LO, is shown in Fig. 10. It is seen from these curves that the zero-current impedance, as well as the reverse impedance, of the detector is $\approx 1.5\,\Omega$. This value, which is very low, is essentially independent of the presence of the LO. Using a calibrated thermopile and the I–V characteristic of Fig. 10, the quantum efficiency and responsivity for the device were directly determined to be 8.5% and 0.9 V/W, respectively. The efficiency could be further improved by depositing an

[60] J. O. Dimmock, I. Melngailis, and A. J. Strauss, *Phys. Rev. Letters* **16**, 1193 (1966).

M. C. Teich, "Coherent Detection in the Infrared," in Semiconductors and Semimetals, vol. 5, Infrared Detectors, edited by R. K. Willardson and A. C. Beer (Academic Press, New York, 1970), ch. 9, pp. 361-407.

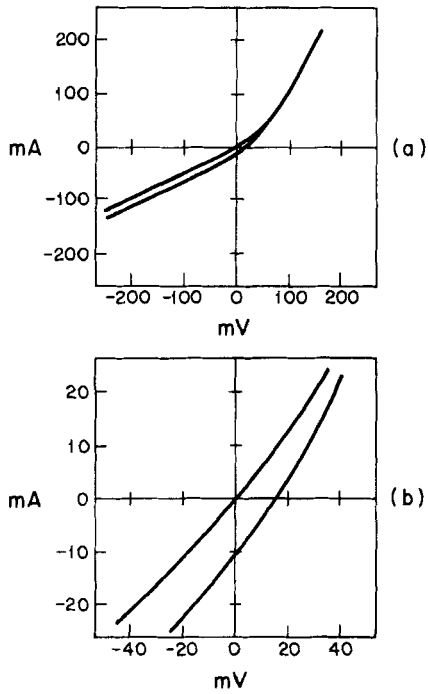

FIG. 10. (a) Current–voltage (I–V) characteristic of the $Pb_{0.936}Sn_{0.064}Se$ diode used in the heterodyne experiments. The upper trace is the dark characteristic, while the lower trace is the characteristic with the (18 mW) LO applied. (b) Same characteristic on expanded I and V scales. (After Teich.[7])

antireflection coating on the diodes. The numerical values for the quantum efficiency and the responsivity are consistent with those obtained by Melngailis using a different method at much lower radiation powers. Improvements in the device characteristics subsequent to the measurements described here are mentioned in the Conclusion.

c. Discussion of Experiment

The arrangement used in the heterodyne experiments (see Fig. 4) was described in detail earlier. A transformer at the output of the detector transformed its impedance to a level appropriate for matching to the low-noise amplifier. The experimental procedure was identical to that described for measurements on Ge:Cu, i.e., various values of the signal beam radiation power P_s were obtained by inserting calibrated CaF_2 attenuators in the signal beam. The unattenuated power was determined from the known responsivity of the diode by chopping the signal beam in the absence of the LO, and then using phase-sensitive detection. In all cases the direct response

M. C. Teich, "Coherent Detection in the Infrared," in Semiconductors and Semimetals, vol. 5, Infrared Detectors, edited by R. K. Willardson and A. C. Beer (Academic Press, New York, 1970), ch. 9, pp. 361-407.

of the detector was ascertained to depend linearly on the LO radiation power. In calculating the signal-to-noise ratio, only noise arising from the presence of the LO was considered. The noise figure of the amplifier was such that with modest LO powers of ~15 mW the noise associated with the LO was typically ~25% of the total noise. It appears that higher LO powers could have been used without any difficulty; however, a rearrangement of the apparatus would have been required to obtain LO powers in excess of the value used.

Experiments were performed in two different regions of heterodyne frequency and bandwidth: an IF of 110 kHz with a bandwidth of 65 kHz, and an IF of 2.05 MHz with a bandwidth of 10.0 MHz. They are described below.

d. Heterodyne Operation at kHz Frequencies

A Princeton Applied Research Model AM-2 input transformer (frequency range 5–150 kHz, turns ratio 1:100) coupled the detector output to the high-input-impedance, low-noise amplifier (PAR Model CR4-A). Measurements were made with an LO power of 9 mW.

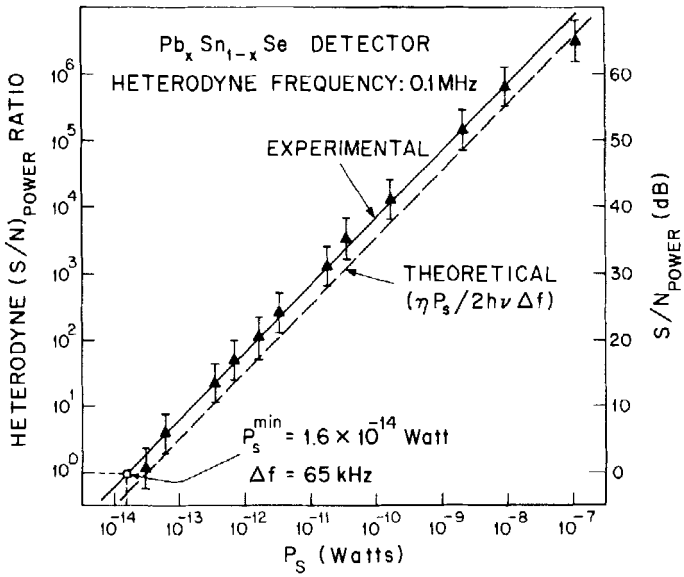

FIG. 11. The solid line is the observed signal-to-noise ratio for the heterodyne signal in $Pb_{1-x}Sn_xSe$ as a function of the signal-beam radiation power. The heterodyne frequency is 110 kHz and the detection bandwidth is 65 kHz. The theoretical curve, $(S/N)_{power} = \eta P_s/2h\nu\,\Delta f$, lies within the limit of experimental accuracy. (After Teich.[7])

M. C. Teich, "Coherent Detection in the Infrared," in Semiconductors and Semimetals, vol. 5, Infrared Detectors, edited by R. K. Willardson and A. C. Beer (Academic Press, New York, 1970), ch. 9, pp. 361-407.

The results of a typical experiment are shown in Fig. 11. The solid line is the observed signal-to-noise power ratio $(S/N)_{power}$ of the heterodyne signal as a function of the signal beam radiation power P_s. With a heterodyne signal centered at 110 kHz and a transformer–amplifier bandwidth of 65 kHz the experimentally observed minimum detectable power P_s^{min} is 1.6×10^{-14} W. The dashed line in Fig. 11 represents the theoretical result. Using the relation $(S/N)_{power} = \eta P_s/2h\nu\,\Delta f$ and a quantum efficiency $\eta = 0.085$, it lies within the limits of experimental accuracy. The observed minimum detectable power corresponds, in a 1-Hz bandwidth, to 2.5×10^{-19} W. Since the experiments were performed using a scattering surface, however, it must be kept in mind that the observation bandwidth for the heterodyne signal must be greater than the noise modulation bandwidth (~50 kHz for an IF of 100 kHz) for an accurate measurement of the signal-to-noise ratio.

e. Heterodyne Detection at MHz Frequencies

The behavior of the $Pb_{1-x}Sn_xSe$ heterodyne detectors at MHz frequencies was investigated by rotating the scattering wheel faster. This was accomplished by replacing the 300-rpm synchronous motor driving the scattering wheel with a 3600-rpm motor. A small matching transformer (turns ratio

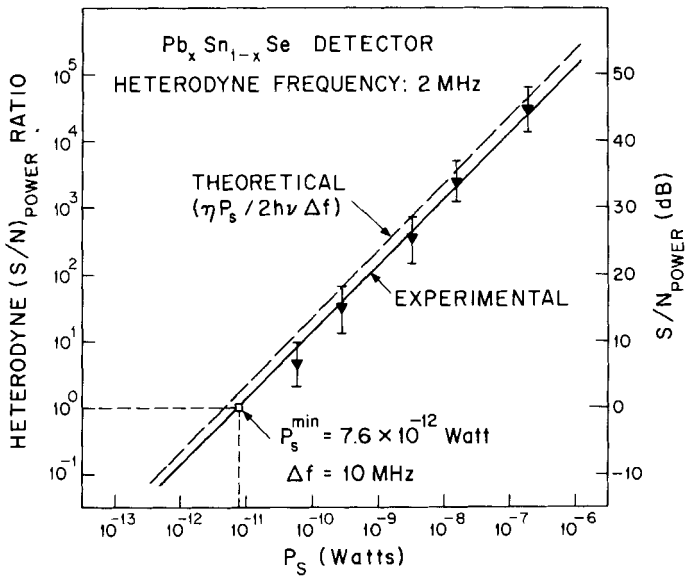

FIG. 12. Signal-to-noise ratio as a function of signal-beam radiation power for 2.05 MHz heterodyne signal from $Pb_{1-x}Sn_xSe$. The agreement of theory and experiment, as in Fig. 11, is good. (After Teich.[7])

M. C. Teich, "Coherent Detection in the Infrared," in Semiconductors and Semimetals, vol. 5, Infrared Detectors, edited by R. K. Willardson and A. C. Beer (Academic Press, New York, 1970), ch. 9, pp. 361-407.

11:55, 30 gauge wire, on a Ferroxcube Corporation 7F160 cup core) at the output of the detector provided an impedance of approximately 50 ohms at the input of a wide-bandwidth, low-noise, integrated-circuit amplifier. The effective bandwidth of the transformer–amplifier combination was 10.0 MHz. The LO power was determined from Fig. 10 (and the known responsivity of the detector) to be 18 mW.

The signal-to-noise ratio for the heterodyne signal at 2.05 MHz is shown in Fig. 12. This plot is similar to that of Fig. 11, except for the IF and the bandwidth. The minimum detectable power for this experiment is 7.6×10^{-12} W, which is larger than that of Fig. 11 because of the increased bandwidth. The dashed line, representing the theoretical result, predicts a value

$$P_s^{\min} \approx 4.8 \times 10^{-12} \quad \text{W}, \tag{43}$$

which is within the experimental bracket. The observed minimum detectable power, extrapolated to a 1-Hz bandwidth, is 7.6×10^{-19} W, which may be compared with the expected value

$$(2/\eta)h\nu\,\Delta f \approx 4.8 \times 10^{-19} \quad \text{W}. \tag{44}$$

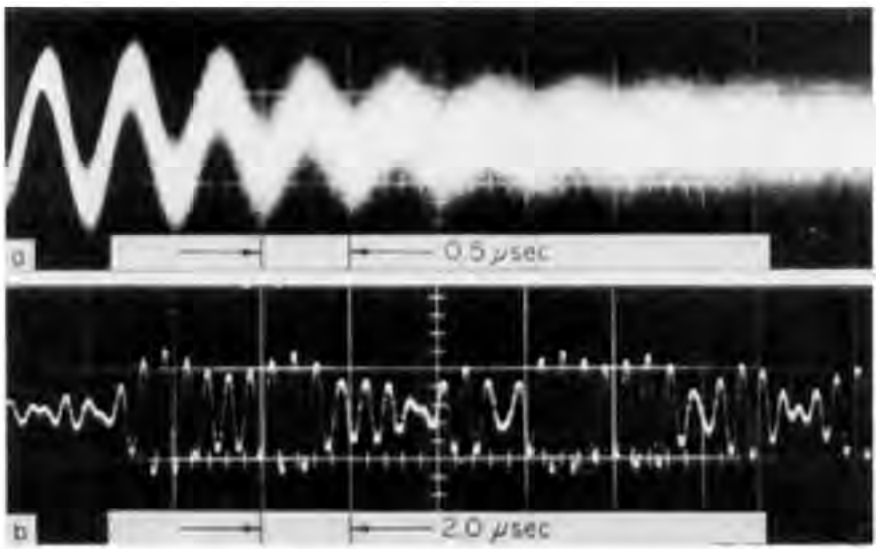

FIG. 13. (a) A multiple-sweep display of the heterodyne signal in $Pb_{1-x}Sn_xSe$. The loss of definition of the waveform in the fifth cycle reflects the finite bandwidth of the signal. (b) A single sweep of the heterodyne signal shown in (a), but with a longer time scale. This figure is similar to Fig. 6 for Ge:Cu; note the very different time scales, however. (After Teich.[7])

M. C. Teich, "Coherent Detection in the Infrared," in Semiconductors and Semimetals, vol. 5, Infrared Detectors, edited by R. K. Willardson and A. C. Beer (Academic Press, New York, 1970), ch. 9, pp. 361-407.

f. Noise Modulation

Figure 13(a) shows a multiple sweep display at the detector output which is similar to that shown for Ge:Cu in Fig. 6. The loss of definition of the waveform in the fifth cycle reflects the finite bandwidth of the heterodyne signal. Figure 13(b) shows a single trace of this signal for a longer time scale. Since the noise modulation bandwidth B and the heterodyne frequency are both proportional to the angular velocity of the scattering wheel $\dot{\theta}$, their ratio is independent of the IF and depends only on geometrical factors. Therefore Figs. 6 and 13 appear very much alike in spite of their very different time scales. This will be discussed quantitatively and in detail in Part IV.

g. Results for $Pb_{1-x}Sn_xTe$

Heterodyne detection has also been observed in $Pb_{1-x}Sn_xTe$ diodes operated in the photovoltaic mode.[56,60a–62] The particular alloy composition used had $x = 0.17$ ($Pb_{0.83}Sn_{0.17}Te$), which has its peak response at 10.6 μ when operated at 77°K. The detector output voltage was observed to be proportional to the square root of the signal beam power ($\propto \sqrt{P_s}$), as is expected for heterodyne operation. The responsivity of these preliminary diodes was too low, however, to observe the noise associated with the LO. This, of course, is necessary for optimum heterodyne detection. Recent advances in the operation of these diodes (see Chapter 4 by Melngailis and Harman) make them appear very suitable for heterodyne detection, however.

IV. Detection from a Moving Diffuse Reflector

Most of the measurements discussed previously have been concerned with a mean detection rate or a time-averaged value of the signal-to-noise ratio. They are therefore related specifically to the first-order coherence properties of the incident radiation. Information other than average count rates, such as the spectral distribution of the mixing signal and the probability density of its envelope, has also been obtained experimentally.[7a] Quantities such as these may be shown to depend on correlation functions[24] of the radiation field higher than first-order, however. Freed and Haus,[39] for example, have related the power-spectral-density of the photocurrent for a direct (non-heterodyne) detector to the second factorial moment of the photocounting distribution, and thus to a second-order correlation function of the radiation

[60a] M. C. Teich, unpublished.

[61] I. Melngailis and A. R. Calawa, *Appl. Phys. Letters* **9**, 304 (1966).

[62] I. Melngailis, A. R. Calawa, J. F. Butler, T. C. Harman, and J. O. Dimmock, Photovoltaic Effect in $Pb_xSn_{1-x}Te$ Diodes, presented at the Intern. Electron Devices Meeting, Washington, D.C., October 26–28, 1966.

M. C. Teich, "Coherent Detection in the Infrared," in Semiconductors and Semimetals, vol. 5, Infrared Detectors, edited by R. K. Willardson and A. C. Beer (Academic Press, New York, 1970), ch. 9, pp. 361-407.

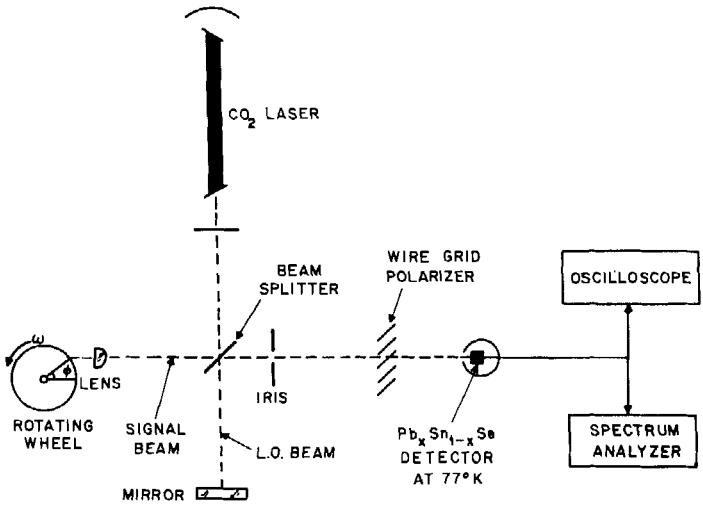

FIG. 14. Experimental arrangement for power-spectral-density and statistical measurements with a lead–tin selenide photovoltaic detector and a sandblasted aluminum scattering wheel. (After Teich.[7a])

field. The spectral-density for the photomixing signal has been considered by Forrester[62a] who obtained an expression for this quantity in terms of the spectral-densities of the light beams, for the case of Gaussian radiation. Mandel[62b] has considered the mixing of two independent *laser* modes and has arrived at an expression similar to that given by Forrester. The spectrum for the heterodyne signal is not *strongly* dependent on the higher-order coherence properties of the individual sources, however.

In this section, the fluctuation properties of the homodyne signal arising from the scattering wheel experiments are discussed. This is generally the configuration of an infrared laser radar, as mentioned previously. In particular, we investigate the power-spectral-density of the heterodyne signal and the probability density of its envelope when the radiation oscillator is fully coherent, i.e., a single-mode stabilized laser operated well above threshold. The parameters we study provide direct information about a target, such as its velocity and its statistical nature. They are also useful in the optimum processing or transmission to a distant point of the heterodyne signal. As a simple example, the signal amplifier should be designed for minimum noise figure, and its bandwidth chosen sufficiently large to pass the heterodyne signal. Such design will, in general, depend upon both the

[62a]A. T. Forrester, *J. Opt. Soc. Am.* **51**, 253 (1961).
[62b]L. Mandel, *Phys. Rev.* **138**, B753 (1965).

M. C. Teich, "Coherent Detection in the Infrared," in Semiconductors and Semimetals, vol. 5, Infrared Detectors, edited by R. K. Willardson and A. C. Beer (Academic Press, New York, 1970), ch. 9, pp. 361-407.

fluctuation and spectral properties of the input signal. Information about the nature of the scattering medium may also be obtained from careful examination of the details of the homodyne signal. This is the basis of the use of the technique for heterodyne spectroscopy. For example, the homodyne return from a moving puff of steam is considerably broader in frequency than the return from a diffusely reflecting moving metallic target, as will be seen later. This results, of course, from the large velocity spread of the constituent water molecules. Further information may be obtained, in a similar way, by studying the probability density of the homodyne signal or its envelope. These quantities are much more strongly dependent on the higher-order correlation functions of the radiation field than is the photomixing spectrum. In fact, the electric field probability distribution of an unknown radiation source may be determined by the heterodyne mixing of this source with a stable oscillator, as will be shown.

We first proceed to describe the details of the experimental arrangement to measure these parameters, and then present our results for the power-spectral-density and probability distribution of the envelope of the homodyne signal.

6. Experimental Arrangement

The experimental arrangement for these measurements is illustrated in Fig. 14. It is quite similar to the arrangement shown in Fig. 4, with the noted absence of certain components required only for measurements of the signal-to-noise ratio. All experiments described in this section were performed with the photovoltaic lead–tin selenide diode.

The output of the detector was fed into a Tektronix type 585A oscilloscope for the probability density measurements, and into a Panoramic type SPA-3a spectrum analyzer for the power-spectral-density measurements. In distinction to experiments designed to measure signal-to-noise ratios, the heterodyne signal was displayed without amplification. In these experiments, the LO power was maintained at a level of approximately 18 mW, while the signal beam radiation power was sufficient ($\gtrsim 10^{-7}$ W) to provide a very high signal-to-noise ratio. The heterodyne signal was centered at about 2.0 MHz and had a mean voltage level of about 0.03 V.

7. Power-Spectral-Density of the Heterodyne Signal

The time trace of a typical heterodyne signal and its envelope, obtained from an oscilloscope photograph, is represented in Fig. 15. It has the appearance of a narrowband random process, i.e.,

$$B/\nu_D < 1, \tag{45}$$

where B is the heterodyne signal frequency bandwidth and ν_D is the heterodyne or Doppler frequency (which is used interchangeably with $\omega_{IF}/2\pi$). The

M. C. Teich, "Coherent Detection in the Infrared," in Semiconductors and Semimetals, vol. 5, Infrared Detectors, edited by R. K. Willardson and A. C. Beer (Academic Press, New York, 1970), ch. 9, pp. 361-407.

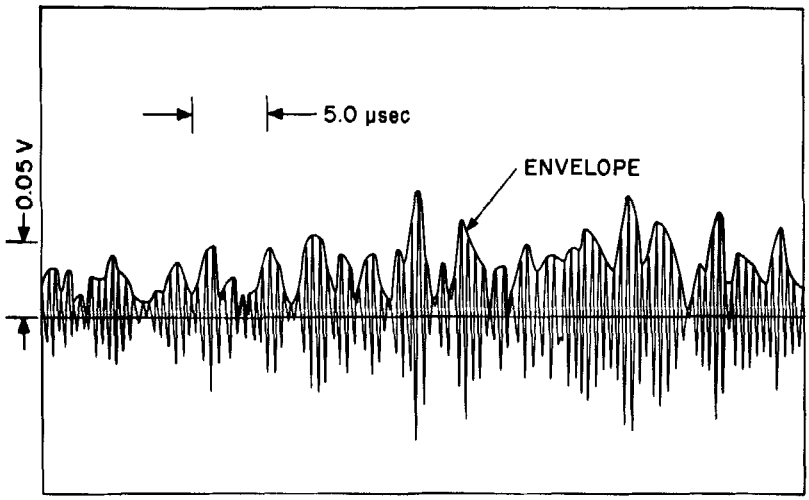

FIG. 15. Time trace of a typical heterodyne signal and its envelope. (After Teich.[7a])

quantities B and B/v_D are easily calculated for 3 cases: (a) focused radiation on the rotating wheel, (b) unfocused radiation on the rotating wheel, and (c) a typical radar experiment.

For a radiation spot of diameter d on the wheel, a completely new area of the wheel is illuminated every $d/v_\perp$ seconds, giving scattered radiation which, as before, we assume to be uncorrelated with that of the previous time interval. It should be pointed out that only the uncorrelated case is considered here, which is equivalent to taking an infinite variance for the surface roughness distribution. This model could be modified (to include a time-dependent mean and a finite variance) in order to allow for a determination of the target's mean path, or surface shape, which might be possible in some applications. Nevertheless, for the uncorrelated case, the heterodyne signal frequency bandwidth may be written as

$$B \approx v_\perp/d. \tag{46}$$

This is a more accurate result than that given previously in Eq. (35). The quantity $v_\perp$ represents the wheel velocity perpendicular to the beam axis, and is equal to $v \cos \phi$ where v is the tangential velocity of the wheel and ϕ is the central angle shown in Fig. 14. Thus, for *focused* radiation, the heterodyne signal bandwidth B_{foc} is given by

$$B_{foc} \approx (r\dot{\theta}D/F\lambda) \cos \phi, \tag{47}$$

which is similar to Eq. (39) but more precise. For any reasonable value of ϕ,

M. C. Teich, "Coherent Detection in the Infrared," in Semiconductors and Semimetals, vol. 5, Infrared Detectors, edited by R. K. Willardson and A. C. Beer (Academic Press, New York, 1970), ch. 9, pp. 361-407.

the contribution to the bandwidth arising from the finite spot size on the scattering wheel may be neglected in this case.

The Doppler frequency ν_D, as is well known, is given by the relationship

$$\nu_D = 2v_{\parallel}/\lambda = (2v/\lambda)\sin\phi, \tag{48}$$

where $v_{\parallel}$ is the wheel velocity component parallel to the radiation beam axis. The ratio of bandwidth to heterodyne frequency B_{foc}/ν_D may then be written

$$B_{foc}/\nu_D \approx (D/2F)\cot\phi. \tag{49}$$

This ratio depends only on geometrical factors, as has been pointed out previously. For moderate values of ϕ, this quantity will be less than or of the order of unity in most cases, although it may be seen that the narrowband nature of the signal will be destroyed for sufficiently small values of ϕ.

For the case of *unfocused* radiation and the rotating wheel, there are two individual contributions to the finite bandwidth: the $v_{\perp}/d$ component as in the last case, and the contribution arising from the spread in Doppler frequencies over the finite spot size on the wheel. We denote this latter quantity by $\Delta\nu_D$. From Eq. (48), it is easily seen that

$$\Delta\nu_D = (2v\,\Delta\phi/\lambda)\cos\phi \tag{50}$$

for the usual case of $\Delta\phi \ll 1$ and thus,

$$\Delta\nu_D/\nu_D \approx \cot\phi\,\Delta\phi. \tag{51}$$

But, since $\Delta\phi$ is given by the relation

$$\Delta\phi \approx d/(r\cos\phi), \tag{52}$$

where d again represents the (unfocused) spot size on the wheel, we obtain

$$\Delta\nu_D/\nu_D \approx (d/r)\csc\phi. \tag{53}$$

The $v_{\perp}/d$ contribution is easily seen to be

$$\frac{v_{\perp}/d}{\nu_D} = (\lambda/2d)\cot\phi, \tag{54}$$

so that the total fractional frequency spread B_{unfoc}/ν_D may be written as

$$B_{unfoc}/\nu_D \approx [(d/r)^2\csc^2\phi + (\lambda/2d)^2\cot^2\phi]^{1/2}. \tag{55}$$

For most situations, this quantity will be smaller than unity for moderate values of ϕ (e.g., for $d/r \sim 0.1$, and $\lambda \ll d$, $B_{unfoc}/\nu_D < 1$ provided only $\phi > 5°$), so that the signal will usually possess a narrowband character in this case as well. Generally for the unfocused case, $\lambda \ll d \ll r$, so that the Doppler-frequency spread will be the dominant term.

M. C. Teich, "Coherent Detection in the Infrared," in Semiconductors and Semimetals, vol. 5, Infrared Detectors, edited by R. K. Willardson and A. C. Beer (Academic Press, New York, 1970), ch. 9, pp. 361-407.

We now consider the return from an infrared *radar* beam tracking a moving solid target. If it is assumed that the beam size d is of the order of the target size, then the frequency broadening arising from the target's diffuse nature will be negligible. But in analogy with the previous case treated, there will be a contribution arising from the *spin* or *rotation* of the target about an axis perpendicular to the beam direction, which gives rise to a Doppler-frequency spread. In this case, then, the center frequency of the mixing signal is given by

$$\nu_D = 2v_{\parallel}/\lambda \tag{56}$$

where now

$$v_{\parallel} = v_r \tag{57}$$

is the radial velocity of the target as a whole. Then, an order-of-magnitude estimate of the bandwidth may be given by

$$B_{radar} \sim 2(2v_{rot}/\lambda) \approx 4r\omega_{\perp}/\lambda, \tag{58}$$

where r is the "radius" of the target, v_{rot} is its rotational velocity, and $\omega_{\perp}$ is the component of angular velocity perpendicular to the beam direction. Therefore, the bandwidth to Doppler frequency ratio may be written as

$$B_{radar}/\nu_D \approx 2r\omega_{\perp}/v_r, \tag{59}$$

which indicates a narrowband signal when $2r\omega_{\perp} < v_r$.

Thus, for the radar configuration discussed, the center frequency of the heterodyne signal determines the radial velocity of the target (v_r) while the bandwidth of the signal may provide information about the spin or rate of rotation of the target. Coupled with the time dependence of the amplitude of the return (reflecting the infrared radar cross section), specific information may also be obtained, in principle, about the surface characteristics and shape of the target. For a beam size which is smaller than the target, on the other hand, one can scan the target to determine its velocity profile and thus its rate of rotation (e.g., the moon). The contributions would be similar to those observed for unfocused radiation falling on the scattering wheel, with the additional consideration that a center-of-mass translational radial velocity will increase the center heterodyne frequency ν_D. Therefore, in analogy with a microwave radar, a good deal more may be learned about a target than just the magnitude of a single one of its velocity components.

The validity of Eqs. (47) and (49) above has been demonstrated experimentally with the rotating scattering wheel. For a 5.05-cm radius wheel rotating at 3600 rpm ($\dot{\theta} = 120\pi\ \text{sec}^{-1}$), with $F = 2.54$ cm, $D \approx 5$ mm, and $\phi \approx 30°$, we calculate the values

$$B_{foc} = 0.3 \pm 0.1 \quad \text{MHz} \tag{60}$$

M. C. Teich, "Coherent Detection in the Infrared," in Semiconductors and Semimetals, vol. 5, Infrared Detectors, edited by R. K. Willardson and A. C. Beer (Academic Press, New York, 1970), ch. 9, pp. 361-407.

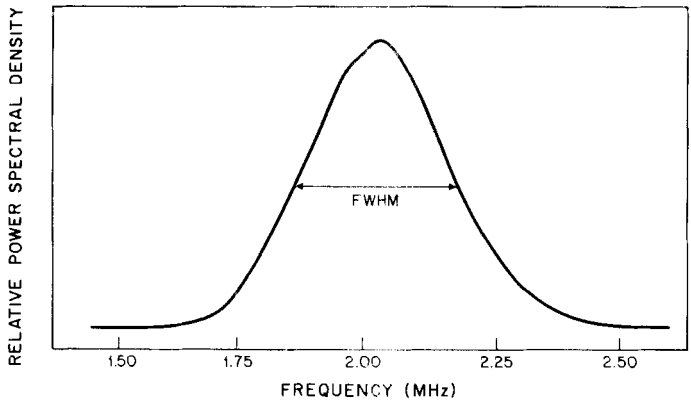

FIG. 16. Experimentally measured power-spectral-density of the heterodyne signal as a function of frequency. Also shown is the full-width at half-maximum (FWHM) of the curve. (After Teich.[7a])

and

$$B_{\text{foc}}/\nu_{\text{D}} = 0.17 \pm 0.05 \tag{61}$$

from Eqs. (47) and (49), respectively. The experimentally measured (relative) power-spectral-density under these conditions is shown in Fig. 16. In this figure, the power-spectral-density scale is linear and the frequency resolution is approximately 0.05 MHz. The measured values of $B_{\text{foc}} = 0.3$ MHz (FWHM) and $B_{\text{foc}}/\nu_{\text{D}} = 0.15$ are in good agreement with the predicted values above. The narrowband nature of the signal for these parameter values is most clearly displayed on a multiple-sweep display such as is shown in Fig. 13a. The loss of definition in the fifth cycle reflects the ratio $B_{\text{foc}}/\nu_{\text{D}}$.

As the angle ϕ is decreased (see Fig. 14), maintaining focusing of the beam on the wheel rim and the same experimental configuration, the number of cycles before loss of definition decreases, reflecting the increasing value of $B_{\text{foc}}/\nu_{\text{D}}$ ($\propto \cot \phi$). For sufficiently small values of ϕ, the narrowband nature of the signal disappears, as expected, and the multiple-sweep display loses all resemblance to the kind of picture seen in Fig. 13a. On the other hand, a *decrease* in the ratio B/ν_{D} has been observed by simply removing the focusing lens from the experimental arrangement leaving ϕ unaltered. This operation had the effect of adding cycles to a representation such as that shown in Fig. 13a. This effect is understood on the basis of Eqs. (49) and (55), keeping in mind that for the unfocused case

$$d/r \gg \lambda/2d, \tag{62}$$

and that d is limited to about 2 mm by the iris aperture for these experiments. The heterodyne signal amplitude may decrease in this case, however, if the

M. C. Teich, "Coherent Detection in the Infrared," in Semiconductors and Semimetals, vol. 5, Infrared Detectors, edited by R. K. Willardson and A. C. Beer (Academic Press, New York, 1970), ch. 9, pp. 361-407.

detector resolves the illuminated spot on the wheel. This has been discussed previously. Analogously, for optimum detection in a real radar experiment, the receiver aperture must be sufficiently small so as not to resolve the return signal,[51,52] in order to maintain spatial coherence.

We have discussed the power-spectral-density of the homodyne signal in terms of the size, granularity, and configuration of the scattering target. It has not been necessary to refer specifically to the coherence properties of the scattered radiation. Such is not the case, however, if we investigate the statistical nature of the heterodyne signal or its envelope. For these parameters, it is necessary to have direct information about the statistical nature of the scattered radiation signal, or about its higher-order correlation functions. This is discussed in the next section.

8. Probability Density of the Signal Envelope

A knowledge of the statistical behavior of the heterodyne signal is useful for the optimum processing and transmission of the signal, as well as for providing information concerning the nature of the scattering medium. Because of the narrowband nature of the homodyne signal in many cases of interest, it is useful (and practically speaking, simpler) to investigate the form of the envelope probability density function. We may then compare the theoretically expected results with those obtained from experiments with a known scatterer, and thus verify the validity of our theoretical model and method of calculation.

It has been shown earlier that double- and sum-frequency heterodyne terms do not appear in the properly formulated quantum theory of infrared heterodyne detection. For radiation fields which possess a positive-definite weight function in Glauber's P-representation,[25] which is the case for all fields considered here, the heterodyne detector response may be written in terms of a semiclassical representation as

$$r_{\mathrm{IF}} \propto \mathscr{L}[E_{\mathrm{LO}} \cos(\omega_{\mathrm{LO}} t) E_{\mathrm{S}} \cos(\omega_{\mathrm{S}} t + \delta)]. \tag{63}$$

Here, as before, r_{IF} represents the photodetector response at the intermediate frequency, E_{LO} and E_{S} represent the magnitude of the electric field for the local oscillator (LO) and the scattered (S) beams, respectively, ω the angular frequency of the particular radiation beam, and δ is a phase angle. The operator $\mathscr{L}$ stands for the "low frequency part of."

Now, if the LO arises from a well-stabilized single-mode laser above threshold, as assumed earlier, then E_{LO} and ω_{LO} are strictly constant. The addition of a constant phase has been omitted for simplicity. The random scattering from the rotating wheel (see Fig. 14) has the effect of converting the "coherent" incident LO radiation to narrowband Gaussian[25] radiation. This conversion of radiation statistics is similar to that obtained by inserting

M. C. Teich, "Coherent Detection in the Infrared," in Semiconductors and Semimetals, vol. 5, Infrared Detectors, edited by R. K. Willardson and A. C. Beer (Academic Press, New York, 1970), ch. 9, pp. 361-407.

a rotating ground-glass screen in the transmission path of a laser beam and is a consequence of the central-limit theorem. Such experiments have been performed by Martienssen and Spiller[62c] to convert deliberately a coherent laser mode to narrowband chaotic radiation in order to observe a positive Hanbury-Brown–Twiss correlation. Thus, the scattered radiation differs from the LO radiation in two respects: its frequency is altered (Doppler shifted), and its statistical properties are changed.

As a consequence, the scattered beam *radiation field* may be represented as a narrowband Gaussian random process (centered in the infrared) and may be written in standard form[62d] as $E_S(t)\cos[\omega_S t + \delta(t)]$. From this, we rewrite r_{IF} as

$$r_{IF} = \beta E_{LO} E_S(t) \cos[|\omega_{LO} - \omega_S| t + \delta(t)]. \tag{64}$$

Since

$$|\omega_{LO} - \omega_S| \equiv \omega_{IF}, \tag{65}$$

we obtain finally

$$r_{IF} = \beta E_{LO} E_S(t) \cos[\omega_{IF} t + \delta(t)]. \tag{66}$$

But this expression for the homodyne *signal voltage* is itself, as well, in the form of a narrowband Gaussian random process. Now, however, it is centered at the Doppler frequency. Nonetheless, although both constituent beams (LO and S) are stationary, optimum *sinusoidal* photomixing is not obtained because the additional requirement of first-order coherence for the total incident field is satisfied only for time intervals well under a coherence time. (The detection has, nevertheless, been shown earlier to be optimum.) It is therefore seen that for an experimental arrangement such as described here, the heterodyning process effectively translates the fluctuation properties of the scattered field down to the Doppler frequency. Stated differently, the heterodyne voltage accurately reflects the scattered beam electric field distribution in a beating experiment performed with an amplitude-stabilized LO without fluctuation. Indeed, another example of this is the mixing of two strong amplitude-stabilized fields. Hinkley *et al.*[62e] have mixed the radiation from a single-mode CO_2 laser with that of a single-mode $Pb_{1-x}Sn_xTe$ semiconductor laser operated well above threshold and obtained a sinusoidal beat signal with almost no fluctuation. The envelope of the heterodyne signal in this case has essentially a delta-function voltage probability distribution, reflecting the absence of amplitude fluctuations, and therefore, the coherent

[62c] W. Martienssen and E. Spiller, *Am. J. Phys.* **32**, 919 (1964).

[62d] W. B. Davenport, Jr. and W. L. Root, "An Introduction to the Theory of Random Signals and Noise," p. 160. McGraw-Hill, New York, 1958.

[62e] E. D. Hinkley, T. C. Harman, and C. Freed, *Appl. Phys. Letters* **13**, 49 (1968).

M. C. Teich, "Coherent Detection in the Infrared," in Semiconductors and Semimetals, vol. 5, Infrared Detectors, edited by R. K. Willardson and A. C. Beer (Academic Press, New York, 1970), ch. 9, pp. 361-407.

nature of the signal beam. However, on reducing the diode laser power and using very careful measurement techniques,[62f] they have been able to measure the linewidth and Lorentzian shape of the heterodyne signal power-spectral-density and thereby directly observe the quantum *phase* fluctuations in a $Pb_{0.88}Sn_{0.12}Te$ diode laser above threshold, thus verifying the form of the Schawlow–Townes formula. We note that while amplitude fluctuations (such as from the scattering wheel) will result in spectral broadening, pure phase or frequency modulation will not be observable in studies of the envelope but will, of course, be evident in the power spectrum. Thus, measurements of the signal statistics and its spectral-density provide complementary information. Hence, information about a scatterer may be obtained if the behavior of the radiation beam incident on the scatterer is known, or the fluctuations of an unknown radiation source may be studied by mixing with a stable LO.

We now direct our attention to the probability density function for the homodyne signal envelope in the case of scattered radiation from the metallic wheel. As is well known, for a narrowband Gaussian random process (NBGRP),[62d] this should be Rayleigh distributed. A typical trace (sample function) of the homodyne signal and its envelope has been shown in Fig. 15. The probability density of interest was experimentally obtained by sampling the envelope at 1.0 μsec time intervals. Some 15 oscilloscope photographs similar to the one represented in Fig. 15 were analyzed in this fashion, providing 754 data points. The envelope voltage was always taken to the nearest 0.01 V. These data are presented in the histogram of Fig. 17 where, on the relative envelope voltage scale, 1 V actually represents 0.01 V.

Also plotted in the same figure is the Rayleigh density function

$$p(V) = (V/\alpha)\exp(-V^2/2\alpha), \tag{67}$$

which, as may be seen by inspection, fits the experimental data very well. This expected fit was confirmed by performing a chi-squared test.[62g] A value of $\chi^2 = 8.28$ with 7 degrees of freedom was obtained, giving a probability $P = 0.3$ that the deviations from the Rayleigh density function would be expected to be greater than those here observed on repeating the series of measurements. This result provides strong evidence that the signal envelope may indeed be fitted by a Rayleigh distribution.

The single parameter α in the distribution $p(V)$ above was chosen by setting the observed average envelope voltage $\langle V_{obs}\rangle$ equal to the average calculated from the Rayleigh distribution $\langle V_{Ray}\rangle$. Performing the average,

$$\langle V_{Ray}\rangle = \int_0^\infty Vp(V)\,dV, \tag{68}$$

[62f] E. D. Hinkley and C. Freed, *Phys. Rev. Letters* **23**, 277 (1969).

[62g] R. D. Evans, "The Atomic Nucleus," p. 774. McGraw-Hill, New York, 1955.

M. C. Teich, "Coherent Detection in the Infrared," in Semiconductors and Semimetals, vol. 5, Infrared Detectors, edited by R. K. Willardson and A. C. Beer (Academic Press, New York, 1970), ch. 9, pp. 361-407.

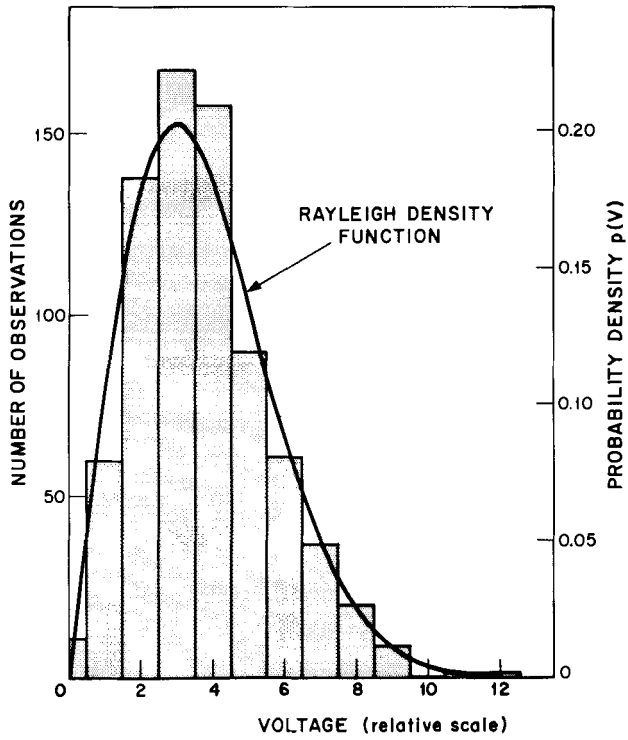

FIG. 17. The heterodyne signal envelope probability density versus voltage. The experimental result (histogram) and the theoretical prediction (Rayleigh density function) are both shown. (After Teich.[7a])

and setting

$$\langle V_{\text{Ray}} \rangle = \langle V_{\text{obs}} \rangle, \tag{69}$$

we obtain

$$\alpha = (2/\pi)\langle V_{\text{obs}} \rangle^2. \tag{70}$$

Thus, taking $\langle V_{\text{obs}} \rangle = 3.73$ relative voltage units from our data (its actual value for the series of experiments performed was 0.0373 V, as may be seen approximately from Fig. 15), we obtain a value

$$\alpha = 8.9 \tag{71}$$

in units of V^2. The particular distribution plotted in Fig. 17 may therefore be written as

$$p(V) = 0.112V \exp(-0.0562V^2). \tag{72}$$

M. C. Teich, "Coherent Detection in the Infrared," in Semiconductors and Semimetals, vol. 5, Infrared Detectors, edited by R. K. Willardson and A. C. Beer (Academic Press, New York, 1970), ch. 9, pp. 361-407.

The most-probable voltage V_p is found from the relation

$$\left.\frac{\partial p(V)}{\partial V}\right|_{V=V_p} = 0, \tag{73}$$

which, for the Rayleigh distribution, gives the prescription

$$V_p = \sqrt{\alpha}. \tag{74}$$

For the experiments described here, $V_p = 2.98$ and $p(V_p) = 0.203$.

These results are consistent with those obtained by Gould *et al.*,[51] who studied the heterodyne signal obtained by scattering visible radiation from different portions of a piece of white bond paper. Finally, it should be mentioned that Goodman has made a detailed comparison of the statistical performance of an optical *energy-detection* radar with a heterodyne radar for pulsed applications.[62h,62i]

V. An Infrared Laser Radar

9. Doppler Radar Configuration

Improved angular resolution and pointing for a radar system may be obtained in the infrared with the use of a laser. Recently a prototype 10.6 μ infrared laser radar has been constructed and operated by Bostick using a Ge:Cu heterodyne detector.[22,63] The experimental arrangement is shown in Fig. 18. The CO_2 laser beam was incident on a modified Michelson interferometer, the conventional leg serving as the LO beam. The other mirror was removed and the (signal) beam was pointed at a target by a plane mirror attached to an inverted radar-type pointing mount on the roof of the laboratory. The laser beam was brought onto the mirror along the fixed axis of the mount in order to preserve an azimuth-elevation system. The system has been operated in the following modes: (1) a position servo loop for fixed directions, (2) manual tracking of moving objects, and (3) an auto-track control loop. The large Dewar containing the Ge:Cu detector, as well as the laser and the modified Mersenne beam expander, may be seen clearly in the photograph of the setup shown in Fig. 19.

10. Radar Results

The return signal from a target is Doppler frequency shifted by an amount $2v_r/\lambda$, where v_r is the radial velocity of the target. At 10.6 μ this is equivalent to about 85 kHz/mph, so that radial velocities of moving objects

[62h] J. W. Goodman, *Proc. IEEE* **53**, 1688 (1965).

[62i] J. W. Goodman, *IEEE Trans. Aero. Elect. Syst.* **2**, 526 (1966).

[63] H. A. Bostick, MIT Lincoln Laboratory, private communication.

M. C. Teich, "Coherent Detection in the Infrared," in Semiconductors and Semimetals, vol. 5, Infrared Detectors, edited by R. K. Willardson and A. C. Beer (Academic Press, New York, 1970), ch. 9, pp. 361-407.

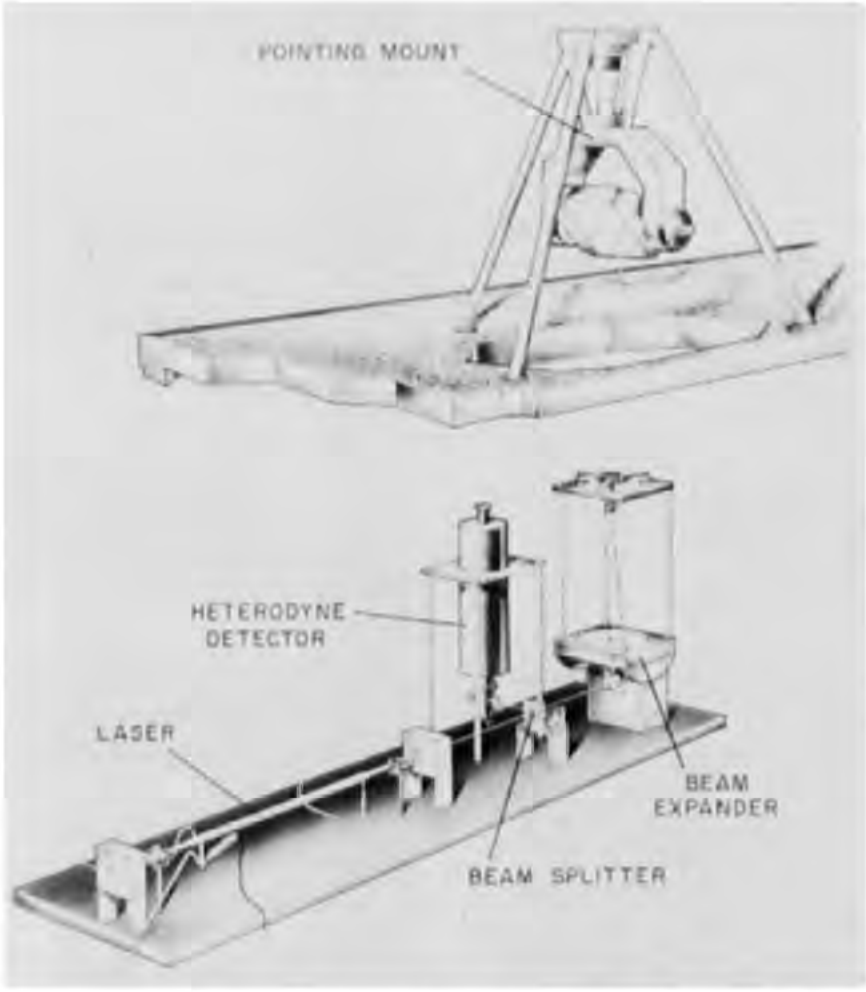

FIG. 18. Drawing of the Doppler-type CO_2 laser radar system. (After Bostick.[63])

such as automobiles and low-flying airplanes may be observed at moderate heterodyne frequencies (below 20 MHz). The large oscilloscope screen (see Fig. 19) is the output of a spectrum analyzer which displays the radar return as a function of frequency.

The tracking of a truck at a range of 1.5 miles is shown in Fig. 20. The vertical axis represents the strength of the heterodyne signal, while the horizontal axis represents the heterodyne frequency. The large spike at the

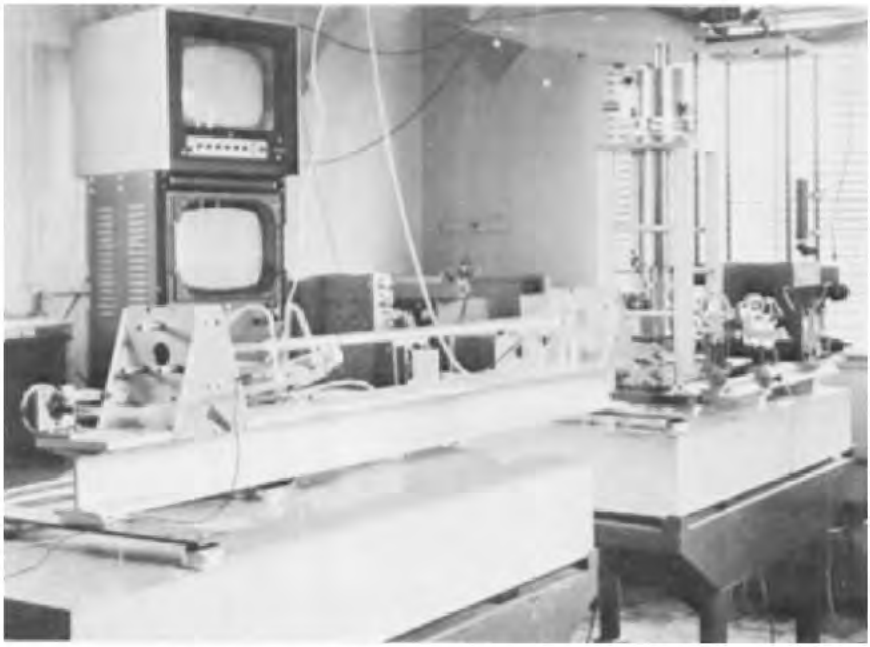

FIG. 19. Photograph of the radar setup. (After Bostick.[63])

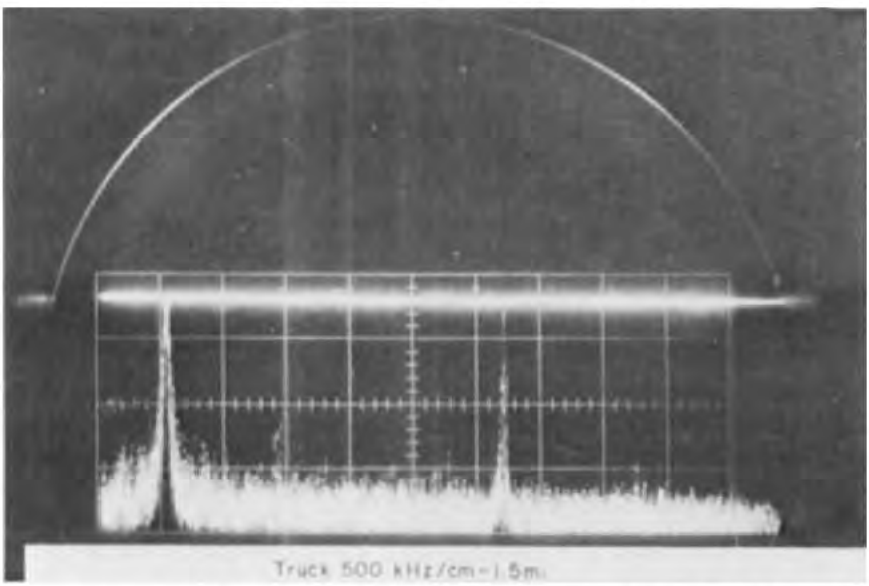

FIG. 20. Radar signal observed from a truck moving with a radial velocity of 32 mph. The range of the truck was 1.5 miles. (After Bostick.[63])

M. C. Teich, "Coherent Detection in the Infrared," in Semiconductors and Semimetals, vol. 5, Infrared Detectors, edited by R. K. Willardson and A. C. Beer (Academic Press, New York, 1970), ch. 9, pp. 361-407.

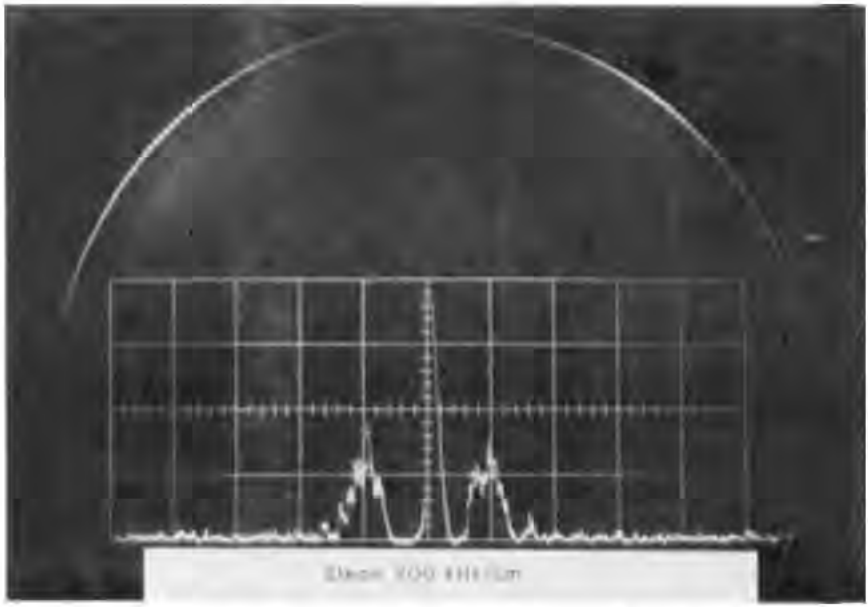

FIG. 21. Radar return from steam. The broad bandwidth of the heterodyne signal reflects the large velocity spread of the constituent water molecules. (After Bostick.[63])

left of the figure represents the zero-frequency beat, while the radar reflection from the truck is seen at 2.7 MHz. The radial velocity of the truck was therefore about 32 mph.[63a] A radar return from steam is shown in Fig. 21. In this case the zero-frequency spike is at the center of the figure, and the upper and lower sidebands of the signal are seen. The average speed of the scattering water molecules is about 2.3 mph, but the broad width of the return reflects the large velocity spread of the constituent molecules. For the solid target, the signal appears to be quite narrowband as discussed earlier.

VI. Photoconductors and Photodiodes in the Infrared: A Comparison

Optimum heterodyne detection has been achieved in the infrared using both photoconductive and photovoltaic detectors. The question of the advantages of each naturally arises.

11. SIGNAL-TO-NOISE RATIO

The signal-to-noise ratio for heterodyne detection was given earlier, where it was shown that for equal quantum efficiency the nonleaky reverse-biased photodiode has a $(S/N)_{\text{power}}$ which is superior to that of the photoconductor

[63a]Since the speed limit in the area was 25 mph, this fellow should have been ticketed!

M. C. Teich, "Coherent Detection in the Infrared," in Semiconductors and Semimetals, vol. 5, Infrared Detectors, edited by R. K. Willardson and A. C. Beer (Academic Press, New York, 1970), ch. 9, pp. 361-407.

and the photovoltaic device by a factor of two. Therefore, from the point of view of S/N it is preferable to operate a (sufficiently high reverse-impedance) diode in a back-biased, rather than in a photovoltaic or photoconductive, configuration. This statement is also valid for direct detection, where the detectivity D^* for reverse-biased operation is augmented by $\sqrt{2}$ over photovoltaic and photoconductive operation.[44] On the other hand, a leaky photodiode characteristic may give rise to adverse effects when operated back-biased, as discussed by Pruett and Petritz.[64]

12. Frequency Response

Aside from the possible improvement in signal-to-noise ratio, another advantage in operating a photodiode in the reverse-biased configuration may be increased frequency response. DiDomenico and Svelto[65] and Lucovsky *et al.*[12] have shown that the frequency response for a heterodyne photodiode is either transit-time or RC limited. Reverse-biasing increases the diode depletion layer, reducing the capacity of the device and therefore increasing its frequency response. (Reducing the carrier density will also decrease the diode capacity.) However, the $Pb_{1-x}Sn_xSe$ photodiodes which were employed had RC time constants ~ 1.5 nsec (with $R \approx 1.5$ ohms and $C \approx 1100$ pF), which was considerably less than the 20-nsec response time. (The response time was measured by connecting the diode directly to a properly terminated 50 ohm line and illuminating it with a 1-nsec risetime GaAs injection-laser pulse.) It is believed that these diodes are presently limited by effective carrier lifetime. This time could be reduced by decreasing the junction depth and therefore the carrier storage time.

Photovoltaic operation may be preferred in certain cases. For example, with diodes having a low reverse impedance a reverse voltage could cause undue heating. In photovoltaic operation the circuitry is simpler,[44] and with low reverse-resistance devices (less than 50 ohms) the use of a broadband transformer might be adequate for impedance transformation and a satisfactory amplifier noise figure for frequencies up to ~ 1 GHz.[66]

For the photoconductor with ohmic contacts the basic frequency response is similar to that of the photodiode; it is lifetime- or RC-limited.[13,65,67] Using fast pulse techniques in 2-mm^3 samples of uncompensated and Sb-compensated Ge:Cu ($C \approx 10$ pF), Bridges *et al.*[68] have recently observed a frequency response of ~ 1 nsec, which is quite close to the RC limit for the

[64] G. R. Pruett and R. L. Petritz, *Proc. I.R.E.* **47**, 1524 (1959).
[65] M. DiDomenico, Jr. and O. Svelto, *Proc. IEEE* **52**, 136 (1964).
[66] C. L. Ruthroff, *Proc. I.R.E.* **47**, 1337 (1959).
[67] O. Svelto, P. D. Coleman, M. DiDomenico, Jr., and R. H. Pantell, *J. Appl. Phys.* **34**, 3182 (1963).
[68] T. J. Bridges, T. Y. Chang, and P. K. Cheo, *Appl. Phys. Letters* **12**, 297 (1968).

M. C. Teich, "Coherent Detection in the Infrared," in Semiconductors and Semimetals, vol. 5, Infrared Detectors, edited by R. K. Willardson and A. C. Beer (Academic Press, New York, 1970), ch. 9, pp. 361-407.

50-ohm system which they used. Similar measurements have been made by Buczek and Picus[50] in the several-hundred-MHz region. It should be mentioned that by proper compensation Ge:Cu detectors with lifetimes as short as 10^{-12} sec have been made.[69] However, it must be kept in mind that when high frequency response is obtained by matching into a 50-ohm system the responsivity of the high-impedance photoconductor is considerably reduced.

13. Device Responsivity

For optimum heterodyne detection it is necessary that the LO be sufficiently strong so as to provide the dominant source of noise (to overcome the amplifier noise). A high responsivity is therefore desirable so that the LO radiation power may be kept moderate. Because the photoconductor responsivity is proportional to the photoconductor gain G, which is given by τ/T, with τ the free-carrier lifetime and T the transit time across the device,[47] it is higher for thin photoconductors. Therefore, a compromise between responsivity and RC frequency response must be made. A discussion of the tradeoffs necessary for optimum photoconductor heterodyne operation at high frequencies ($\rightarrow$ 2 GHz) has been given by Arams *et al.*[70] and is also discussed by them in Chapter 10 of this volume. Thin Ge:Cu detectors have been fabricated for this purpose. On the other hand, photodiodes having high reverse-impedances should have high responsivity, and, since the gain is unity, should in general require less LO than the photoconductor.

14. Temperature of Operation

Finally, perhaps the most striking characteristic of the $Pb_{1-x}Sn_xSe$ (as well as the $Pb_{1-x}Sn_xTe$ and $Cd_xHg_{1-x}Te$) photodiode detectors is their ability to operate well at liquid nitrogen temperatures (77°K). By contrast, Ge:Cu requires near liquid helium temperatures (4°K), while Ge:Hg requires liquid hydrogen temperatures (18°K). The diodes are therefore more convenient to operate and more suitable for field use than are the photoconductors. Nevertheless, the quantum efficiency of the photodiode reported in this work is below that of the photoconductor by a factor of about four, and the minimum detectable power is therefore correspondingly higher. In recent work, however, Melngailis[71] has described $Pb_{1-x}Sn_xTe$ diodes with external quantum efficiences of almost 50%, which is the reflection-limited maximum. The minimum detectable power

[69] R. J. Keyes, MIT Lincoln Laboratory, private communication.

[70] F. Arams, E. Sard, B. Peyton, and F. Pace, *IEEE J. Quantum Electron.* **3**, 241 (1967).

[71] I. Melngailis, Laser Action and Photodetection in Lead–Tin Chalcogenides, presented at the Intern. Colloq. IV–VI Compounds, Paris, July 15–18, 1968.

M. C. Teich, "Coherent Detection in the Infrared," in Semiconductors and Semimetals, vol. 5, Infrared Detectors, edited by R. K. Willardson and A. C. Beer (Academic Press, New York, 1970), ch. 9, pp. 361-407.

for both the $Pb_{1-x}Sn_xTe$ and the Ge:Cu detectors should thus be comparable.

Both photoconductors and photodiodes are seen to be useful for infrared heterodyne detection, the choice of a particular device depending on the desired application.

VII. Conclusion

Heterodyne techniques, which have been used extensively in the radio wave and microwave regions, and more recently in the optical (visible) portion of the electromagnetic spectrum, are equally as valuable in the infrared. The availability of the high power CO_2 laser, coupled with the 8–14 μ atmospheric window, is expected to make the infrared heterodyne receiver important for communications applications. It is more sensitive than the optical heterodyne receiver because of the smaller photon energy (the minimum detectable power is proportional to the photon energy). An infrared heterodyne radar system has been operated. A truck was tracked and its radial velocity determined at a range of 1.5 miles. In recent work, returns from helicopters and airplanes have also been obtained. The technique might also prove useful for infrared heterodyne spectroscopy experiments.

The quantum theory of heterodyne detection in the optical and infrared has been discussed and compared with the classical theory. An important result which obtains from the quantum treatment is the absence of sum- and double-frequency components ($2\omega_1$, $2\omega_2$, and $\omega_1 + \omega_2$) from the heterodyne signal. This is in distinction to the classical result. A condition for optimum photomixing is that the total radiation field incident on the detector possess first-order coherence. It has been shown that heterodyne detection may be interpreted as a process in which a single nonmonochromatic photon is annihilated. The theory applies for fields of arbitrary statistical properties.

In accordance with the theory, theoretically optimum infrared coherent detection has been achieved at kHz heterodyne frequencies using liquid-helium cooled, copper-doped germanium detectors. Detailed considerations pertaining to the detector properties for coherent and incoherent applications have been given by Keyes and Quist in Chapter 8. Lead–tin chalcogenide photovoltaic detectors at liquid nitrogen temperatures have also been operated optimally at kHz and MHz heterodyne frequencies. The incoherent detection aspects of these devices are discussed by Melngailis and Harman in Chapter 4. They are presently effective to wavelengths considerably beyond 10 μ, and have external quantum efficiencies approaching 50%. The responsivity of a $Pb_{0.936}Sn_{0.064}Se$ diode has reached 3.5 V/W at 77°K. These detectors have been operated at dry-ice temperatures (195°K) with a response which is down by only a factor of 20 from its value at 77°K.

M. C. Teich, "Coherent Detection in the Infrared," in Semiconductors and Semimetals, vol. 5, Infrared Detectors, edited by R. K. Willardson and A. C. Beer (Academic Press, New York, 1970), ch. 9, pp. 361-407.

Furthermore, diodes such as $Cd_xHg_{1-x}Te$[72] (which peak at 10.6 μ with $x = 0.195$) and $Pb_{1-x}Sn_xTe$[71] have now been fabricated with reverse-impedances in excess of 50 ohms, so that impedance matching is less of a problem. With the availability of these higher impedances at the amplifier input an added advantage is that the noise figure of the amplifier is improved, thus requiring less LO to overcome amplifier noise. In addition, if the diode reverse-impedance reaches a level where it is much greater than the load resistance, an additional factor of two can be gained in the signal-to-noise ratio with reverse-biased operation.

The "higher-order" properties of the infrared heterodyne signal are useful either in the processing of a known signal, or in obtaining information about an unknown target or signal which cannot be obtained from measurements of average signal values. Expressions for the ratio of heterodyne signal bandwidth to Doppler frequency have been obtained for both focused and unfocused radiation incident on a diffuse wheel, as well as for a typical infrared radar configuration. Agreement with experiments using a focused radiation beam was good. Knowledge of the center frequency, bandwidth, and time-dependence of an infrared radar signal provides information about the radial velocity, spin, surface properties, and shape of the target. Information is also contained in the statistics of the heterodyne signal. The envelope probability distribution for radiation scattered from a rotating diffuse wheel was found to be Rayleigh distributed.

In short, infrared heterodyne detection is now a well-understood process and appears to have a good deal of potential in the fields of communication, radar, and infrared physics. Its application and use in more complex configurations than those presented here is therefore certain to follow. A *three-frequency* mixing scheme, for example, has recently been proposed as advantageous in the acquisition and tracking of radar (or communications) signals when the target (or transmitter) velocity is either unknown or changing rapidly.[73]

ACKNOWLEDGMENTS

I wish to thank I. Melngailis for supplying the $Pb_{1-x}Sn_xSe$ and $Pb_{1-x}Sn_xTe$ detectors used in the experiments reported in this chapter, and to acknowledge many valuable discussions with him, with R. J. Keyes, and with R. H. Kingston. I am grateful to C. H. Townes for the use of his unpublished figure (Fig. 1), and to H. A. Bostick for permission to use Figs. 18–21, which are also unpublished.

[72] C. Vérié and A. Ayas, *Appl. Phys. Letters* **10**, 241 (1967).
[73] M. C. Teich, *Appl. Phys. Letters* **15**, 420 (1969).

M. C. Teich, "Coherent Detection in the Infrared," in Semiconductors and Semimetals, vol. 5, Infrared Detectors, edited by R. K. Willardson and A. C. Beer (Academic Press, New York, 1970), ch. 9, pp. 361-407.